

**SEISMIC ANALYSIS USING WAVELET TRANSFORM FOR HYDROCARBON  
DETECTION**

A Thesis

by

RUI CAI

Submitted to the Office of Graduate Studies of  
Texas A&M University  
in partial fulfillment of the requirements for the degree of

MASTER OF SCIENCE

December 2010

Major Subject: Geophysics

Seismic Analysis Using Wavelet Transform for Hydrocarbon Detection

Copyright 2010 Rui Cai

**SEISMIC ANALYSIS USING WAVELET TRANSFORM FOR HYDROCARBON  
DETECTION**

A Thesis

by

RUI CAI

Submitted to the Office of Graduate Studies of  
Texas A&M University  
in partial fulfillment of the requirements for the degree of

**MASTER OF SCIENCE**

Approved by:

Chair of Committee,  
Committee Members,

Head of Department,

Yuefeng Sun  
Luc T. Ikelle  
Jim Xiuquan Ji  
Andreas Kronenberg

December 2010

Major Subject: Geophysics

## **ABSTRACT**

Seismic Analysis Using Wavelet Transform for Hydrocarbon

Detection. (December 2010)

Rui Cai, B.S., Texas A&M University

Chair of Advisory Committee: Dr. Yuefeng Sun

Many hydrocarbon detection techniques have been developed for decades and one of the most efficient techniques for hydrocarbon exploration in recent years is well known as amplitude versus offset analysis (AVO). However, AVO analysis does not always result in successful hydrocarbon finds because abnormal seismic amplitude variations can sometimes be caused by other factors, such as alternative lithology and residual hydrocarbons in certain depositional environments. Furthermore, not all gas fields are associated with obvious AVO anomalies. Therefore, new techniques should be applied to combine with AVO for hydrocarbon detection. In my thesis, I, through case studies, intend to investigate and validate the wave decomposition technique as a new tool for hydrocarbon detection which decomposes seismic wave into different frequency contents and may help identify better the amplitude anomalies associated with hydrocarbon occurrence for each frequency due to seismic attenuation.

The wavelet decomposition analysis technique has been applied in two geological settings in my study: elastic reservoir and carbonate reservoir. Results from both cases indicate that the wavelet decomposition analysis technique can be used for

hydrocarbon detection effectively if the seismic data quality is good. This technique can be directly applied to the processed 2D and 3D pre-stack/post-stack data sets (1) to detect hydrocarbon zones in both clastic and carbonate reservoirs by analyzing the low frequency signals in the decomposed domain and (2) to identify thin beds by analyzing the high frequency signals in the decomposed domain. In favorable cases, the method may possibly help separate oil from water in high-porosity and high-permeability carbonate reservoirs deeply buried underground. Therefore, the wavelet analysis would be a powerful tool to assist geological interpretation and to reduce risk for hydrocarbon exploration.

## **ACKNOWLEDGEMENTS**

I would like to thank my committee chair, Dr. Sun, and my committee members, Dr. Ikelle, Dr. Jim Ji for their guidance and support throughout the course of this research.

Thanks also go to my friends and colleagues and the department faculty and staff for making my time at Texas A&M University a great experience.

Finally, thanks to my mother and father for their encouragement during my research studies.

## TABLE OF CONTENTS

	Page
ABSTRACT .....	iii
ACKNOWLEDGEMENTS .....	v
TABLE OF CONTENTS .....	vi
LIST OF FIGURES .....	viii
LIST OF TABLES .....	xi
 CHAPTER	
I      GENERAL INTRODUCTION .....	1
1.1 Introduction .....	1
1.2 Theory of wavelet decomposition analysis .....	3
1.3 Statement of the problems .....	4
1.4 Objectives .....	5
1.5 Method .....	5
1.6 Anticipated results and significant impact .....	7
1.7 Thesis structure .....	8
 II      THEORY OF WAVELET TRANSFORM .....	 10
2.1 Introduction .....	10
2.1.1 General information .....	10
2.1.2 History .....	11
2.1.3 Wavelet theory .....	11
2.1.4 The continuous wavelet transform .....	12
2.2 Prototype wavelets .....	14
2.2.1 Morlet wavelet .....	14
2.2.2 Mexican hat (Ricker) wavelet .....	15
2.3 Time-frequency analysis of wave signals .....	16
2.4 Comparison of different mother wavelets .....	20
2.5 Parameter selection for Morlet wavelet .....	22

CHAPTER	Page
2.6 Conclusion.....	25
III SEISMIC ANALYSIS BY USING WAVELET TRANSFORM: THE CLASTIC RESERVOIR CASE IN THE NORTH SEA.....	26
3.1 Introduction .....	26
3.1.1 Geological background of North Sea area .....	26
3.1.2 Testing well information .....	28
3.2 Seismic data analysis by using wavelet transform .....	29
3.2.1 Wavelet analysis for synthetic trace at well location .....	29
3.2.2 Wavelet analysis for real seismic data at well location.....	33
3.2.3 Seismic cross section generated by using wavelet transform	36
3.3 Conclusion.....	42
IV APPLICATION ON ORDOVICIAN FOSSIL KARST FRACTURE CAVITY RESERVOIR.....	44
4.1 Introduction .....	44
4.1.1 Geological background .....	44
4.1.2 Basic concept of using wavelet analysis for karst reservoir..	45
4.2 Wavelet decomposition analysis for karst carbonate reservoir .....	47
4.2.1 Trace analysis using wavelet transform .....	47
4.2.2 3-D seismic data analysis using wavelet transform.....	51
4.3 Conclusion.....	61
V CONCLUSIONS .....	71
REFERENCES .....	74
VITA .....	76



## LIST OF FIGURES

	Page
Figure 2.1 Waveform of the Morlet wavelet.....	14
Figure 2.2 Waveform of the Mexican hat wavelet.....	15
Figure 2.3 The sine waveform for $x=\sin(40*2*\pi*t)$ on range of $[0, 3]$ .....	17
Figure 2.4 The wavelet decomposition for the sine function $x=\sin(40*2*\pi*t)$ shown in Figure 2.3 .....	18
Figure 2.5 The sine function with varying amplitude .....	19
Figure 2.6 The wavelet decomposition for the testing sine function with varying amplitude.....	20
Figure 2.7 The spectrogram of using Mexican hat wavelet .....	21
Figure 2.8 The spectrogram of using Morlet wavelet .....	21
Figure 2.9 The spectrogram with $F_c=0.2$ Hz .....	23
Figure 2.10 The spectrogram with $F_c=5$ Hz .....	23
Figure 2.11 The spectrogram with $F_c=1.5$ Hz .....	24
Figure 2.12 The spectrogram with $F_c=1$ Hz .....	24
Figure 3.1 Overview of North Sea area.....	27
Figure 3.2 Seismic line after stack for North Sea data.....	28
Figure 3.3 Synthetic data trace construction shown in depth.....	30
Figure 3.4 Center frequency selection and well seismic tie.....	31
Figure 3.5 The oil & gas information at Well-A location .....	32
Figure 3.6 Spectrogram for a synthetic seismic trace .....	32
Figure 3.7 The oil & gas diagram in real time at Well-A location.....	33

	Page
Figure 3.8 Spectrogram for real seismic trace at Well-A location.....	34
Figure 3.9 The oil & gas information at Well-B location .....	35
Figure 3.10 Spectrogram for real seismic trace at Well-B location .....	35
Figure 3.11 The 3-D Diagram of decomposed cross section .....	37
Figure 3.12 Cross section spectrogram at 10Hz .....	38
Figure 3.13 Cross section spectrogram at 15Hz .....	39
Figure 3.14 Cross section spectrogram at 20Hz .....	40
Figure 3.15 Cross section spectrogram at 45Hz .....	41
Figure 4.1 Basic structure of Ordovician Karst fracture-cavern reservoir .....	45
Figure 4.2 Cross section for Ordovician fracture cavity reservoir with testing well information .....	48
Figure 4.3 Spectrogram for seismic trace at Well-1 location.....	49
Figure 4.4 Spectrogram for seismic trace at Well-2 location.....	50
Figure 4.5 Spectrogram for seismic trace at Well-3 location.....	51
Figure 4.6 The seismic data information.....	52
Figure 4.7 Cross section with Well-A and Well-A-CH location information.....	53
Figure 4.8 Xline cross section with Ordovician reservoir information in red box and high amplitude in green circle .....	54
Figure 4.9 Cross section spectrogram with using $F_c=0.2$ .....	55
Figure 4.10 Cross section spectrogram of 20 Hz with well information .....	56
Figure 4.11 Cross section spectrogram of 70 Hz with well information .....	57
Figure 4.12 Inline cross section with Well-A location information.....	58

	Page
Figure 4.13 Inline cross section spectrogram of 20 Hz.....	59
Figure 4.14 Inline cross section spectrogram of 70 Hz.....	59
Figure 4.15 Time slice spectrogram at 840 ms with 20 Hz frequency.....	60
Figure 4.16 Time slice spectrogram at 890 ms with 20 Hz frequency.....	61
Figure 4.17 Cross section spectrogram of 20 Hz .....	62
Figure 4.18 Cross section spectrogram of 25 Hz .....	63
Figure 4.19 Cross section spectrogram of 30 Hz .....	64
Figure 4.20 Cross section spectrogram of 35 Hz .....	65
Figure 4.21 Cross section spectrogram of 40 Hz .....	66
Figure 4.22 Cross section spectrogram of 45 Hz .....	67
Figure 4.23 Cross section spectrogram of 50 Hz .....	68
Figure 4.24 Cross section spectrogram of 60 Hz .....	69
Figure 4.25 Cross section spectrogram of 70 Hz .....	70

**LIST OF TABLES**

	Page
Table 4. 1    Testing well information .....	52

## **CHAPTER I**

### **GENERAL INTRODUCTION**

#### **1.1 Introduction**

Energy is an eternal topic for human being. Energy that supports human activities is mainly generated from the conventional energy source: oil and gas. Oil and gas are widely used for fuel production and electricity generation, and their derivatives, such as lubricant, wax, plastic and etc, also play a significant role for modern industry. The whole petroleum industry has supplied the energy for the rapid development of human society. However as the human population grows, energy demands will exceed world's existing supply. Geoscientists need to find new ways to find more deep reserves and to recover more from existing mature fields. Among many challenges, accurate prediction of hydrocarbon occurrence in deep basins is increasingly more important than others in order to reduce drilling risk and economic cost.

Many hydrocarbon detection techniques have been developed in the last several decades. One of the most efficient techniques for hydrocarbon exploration in recent years is amplitude versus offset analysis (AVO). In the 1960s, geophysicists discovered that the high seismic amplitude always appear when the gas exist in clastic reservoir. The geoscientists thought that it would be simple to locate the hydrocarbon zone by finding high light spot in seismic cross section. However, the fact is that the high light spot could be caused by other factors such as coal bed, igneous rock intrusion, and thin-

---

This thesis follows the style and format of Geophysics.

bed tuning. Therefore, geoscientists continued searching methods that can identify hydrocarbon zones by using seismic data. Until 1980s, Ostrander observed some abnormal event that reflecting energy increases as the distance increases between the source and the receiver, namely seismic amplitude increases as the offset increases. Then he delivered the point of view that gas filled clastic reservoir is the reason of causing this abnormal event. And this discovery represented the appearance of AVO technique. This technique then became a very hot topic and had been successfully applied for hydrocarbon detection. Most oil companies use AVO as a tool to lower the risk in exploration process.

However, AVO analysis does not always work because the abnormally rising or falling amplitudes can sometimes be caused by other factors, such as alternative lithology and residual hydrocarbons in certain depositional environment. Furthermore, not all gas fields are associated with obvious AVO anomalies. Therefore, new techniques should be applied to combine with AVO for hydrocarbon detection. Under this circumstance, the wave decomposition technique became the new direction for hydrocarbon detection due to it's widely usage in the field of high frequency digital signal processing. This technique could separate the seismic wave in different frequency contents and detect the amplitude anomaly for each frequency.

There are three major types of wave decomposition methods in digital signal processing: Fourier transform, short Fourier transform and wavelet transform. The seismic wave is a frequency-varying and non-periodic traveling wave, which is classified as non-stationary wave by definition. And in order to sense the seismic wave

anomaly more accurately, the wavelet transform decomposition method which can handle the nonstationary wave better than other two methods will be used in my feasibility studies for hydrocarbon detection.

## **1.2 Theory of wavelet decomposition analysis**

The Fourier transform is a method widely used for many scientific purposes. However, it is only suited for stationary signals of which frequency contents do not change with time.

By using the Fourier transform, the result gives only global information, but it is not suitable for detecting compact patterns. In order to overcome this limitation, the short time Fourier transform has become a conventional method of time-frequency analysis for non-stationary seismic signals. However, the non-stationary seismic wave has varying frequency content in time. By using a pre-defined filter window length, the short time Fourier transform has limitations regarding to the time-frequency resolution (Zabihiand and Siahkookhi, 2006),. Therefore, the decomposition method with a self-adjusted window has become a new research topic for seismic wave analysis. It is achieved by using the continuous wavelet transform, which is one of the most popular methods in signal processing for non-stationary signal decomposition (Sun and Castagna, 2006).

The continuous wavelet transform does not require preselecting a window length. Convolvering a signal with a self-adjusted wavelet is the core concept in this methodology (Goswami and Chang, 1999). As a result, the continuous wavelet transform has become a

powerful tool in non-stationary signal analysis. In wavelet transform, the scale represents the frequency range but not a single frequency, and the location is associated with a sample position but not a time. A location-scale map can be produced with a continuous wavelet transform. Then a time-frequency map can be built by converting the location to time and converting the scale to frequency (Sinha, 2002).

The wavelet transform method was first mentioned by Haar (1910) but was developed by Goupillaud et al. (1984). The application of the wavelet transform to the oil and gas industry was mainly focused on improving the resolution in recent years (e.g., Devi and Schwab, 2009). However, this technique can also be used as a hydrocarbon indicator based on the fact that the basic unit of the seismic signal is a wavelet (e.g., Devi and Cohen, 2004). As long as the seismic wave signal goes through a hydrocarbon zone, there will be a significant anomaly appears on the bottom of reservoir depending on the energy absorption characteristics of the pore fluid (Sato, 1997).

The aim of my research is to investigate the effectiveness of wavelet decomposition as a seismic signal analysis tool for hydrocarbon detection and possibly fluid type classification.

### **1.3 Statement of the problems**

The wavelet decomposition method has begun to be used for seismic data processing in past decades. And more and more geophysicists started to use this technique for geological interpretation with focus on the hydrocarbon detection studies (Sinha, Routh, Anno, and Castagna, 2002). However, this technique is still not widely



applied for oil and gas exploration as a conventional tool of interpretation. Whether this technique is a suitable method for hydrocarbon detections in in-situ field conditions and which wavelet has better performance are still questionable for the wavelet decomposition analysis. Therefore, I will focus these problems in my study, and discuss the applications and limitations of this new technique.

#### **1.4 Objectives**

My research will focus on evaluating how to use better wavelet transform method as a hydrocarbon detection tool and handle the non-stationary seismic signal in field data applications. By applying the wavelet transform method I will analyze seismic data from both geophysical and geological perspectives. The major purpose of my research will apply the wavelet transform to locate hydrocarbon zones from seismic data. In order to achieve my goal, a time-frequency cross-section from real seismic data will be constructed by using the wavelet transform methodology. The hydrocarbon zone, if any, can be shown as a bright spot on the 2-D cross section spectrogram. It can also be understood as an energy distribution diagram based on the fact that the hydrocarbon zone has a high absorption of energy.

#### **1.5 Method**

It is often observed in the field that seismic waves lose high-frequency content when they propagate through a hydrocarbon reservoir. Furthermore, the low frequency part of the seismic wave usually has amplitude resonance with the natural frequency of

hydrocarbon zone. But a few methods exist to detect accurately this information in seismic data. This research mainly focuses on the application of wavelet transform to seismic data for hydrocarbon detection, integrating geology, rock physics, geophysics and the signal processing approach and using seismic data and log data. First, I will investigate how different wavelets affect the performance of wavelet transform on hydrocarbon detection at well locations with proven oil/gas reservoirs. I will identify the time-frequency attributes in the wavelet transform spectrum that can be correlated to known hydrocarbon occurrence at the well locations. Then I will apply the method to field 2-D or 3-D seismic data for both clastic and carbonate reservoirs.

In the first part of my research, I will summarize the mathematical background of wavelet transform in the context of seismic application. Morlet wavelet has frequently used in wavelet transform. However, the Ricket wavelet (the Mexican hat) has been used more commonly in seismic data processing and interpretation. Conversion of the scale parameter in the wavelet transform domain to frequency is not straightforward. I will use a sine function with a constant frequency as an input to wavelet transform to define the scale-to-frequency calibration. I will also use a sine function as an input to test the different wavelets for verification of their validity for seismic applications.

In the second part of my research, I will apply the method to a North Sea dataset to test its effectiveness in detecting hydrocarbon zones. First of all, I will test the method at the well location based on known lithology information, rock physical properties and locations of the hydrocarbon zones from the well log data. A synthetic seismic trace at well location will be constructed to link the well log data to real seismic data. Only

primary seismic waves will be generated in synthetic seismic trace with no multiples. The wavelet transform result will be applied to the synthetic trace to check its validity. Then I will apply the wavelet transform decomposition method to real seismic data trace at the same well location. The real seismic data trace with multiples will be used to detect the effect of multiples on the performance of the wavelet transform for hydrocarbon detection. The wavelet transform result will be compared with the one from synthetic data to help me to indentify the similarity and differences around hydrocarbon reservoir. The wavelet transform method will also be tested using a dataset from a paleo-karst carbonate reservoir.

The third part of my research will focus on the construction of a 2-D time – frequency cross section. I will build 2-D cross section diagram for both the siliciclastic reservoir in the North Sea, and the paleo-karst carbonate reservoir. The wavelet transform decomposition method will be applied to all the traces in the data set with normal incident angle used to construct the 2-D time-frequency cross section diagram, which could be tied to the real structure model, and to show the hydrocarbon zones under a certain signature frequency.

### **1.6 Anticipated results and significant impact**

This research will provide me a more effective way to handle non-stationary seismic wave data and to predict hydrocarbon zones by using the wavelet transform decomposition method for the studied reservoirs. To detect hydrocarbons directly from seismic data has been one of the major challenges in hydrocarbon exploration. The expected research results from this study are as follows:

1. To demonstrate the seismic data are nonstationary based on the time frequency spectrogram.
2. To identify the optimal wavelets that could be best used for finding hydrocarbons or mixed-fluid zones from real seismic data.
3. To develop a methodology of how to better use wavelet transform to detect hydrocarbon zone from real seismic data.
4. To develop a method for interpretation of the wavelet transform decomposition signatures based on time-frequency cross section diagram.
5. To document the limitations of the wavelet transform decomposition method in seismic applications, if any.

If the method developed in this thesis is successfully, it could also be used in other shallow or deep environments at both clastic and carbonate reservoirs. Especially in paleo-karst systems where no well logs are available; this method could play an important role in hydrocarbon prediction before drilling for exploration. Furthermore, it is possible to tie the lithology with frequency by using this method, which could be a benefit in predicting subsurface reservoir rock types using seismic data.

### **1.7 Thesis structure**

In my research, I will focus on applying wavelet analysis techniques to two types of reservoir: both clastic and carbonate. The resulting cross section spectrograms would help the geological interpretation for hydrocarbon detection, and lithology identification based on different decomposition signatures.

In this chapter, I introduce the background information of the evolvement of hydrocarbon detection techniques, and the motives of using wavelet decomposition method for hydrocarbon detection. Furthermore, I outline the challenges encountered in oil and gas exploration and the possible solutions during this research.

In Chapter II, I will provide more detail information about the wavelet transform method. The detail properties of wavelet transform will be introduced in this chapter. A demonstration of converting scale to frequency will be given so that the time-frequency analysis could become available for assisting hydrocarbon detection.

In Chapter III, preliminary results of applying wavelet decomposition analysis to pre-stack seismic data for clastic reservoir in North Sea will be presented. During the analyzing procedure, decomposition signature identification will be focused for further wavelet decomposition study.

The structure of Chapter IV will be similar to Chapter III. However, the significant changes will be in reservoir type and the seismic data quality. With North Sea raw data in Chapter III, verification of wavelet decomposition as a hydrocarbon detection technique is comprised because of the effect of multiples and noise. But the good quality of the processed seismic data in Chapter IV will enable me to provide strong evidences of wavelet transform based spectral decomposition as a successful method for hydrocarbon detection.

In Chapter VI will conclude all my studies. The limitations of proposed methods will also be discussed in this chapter.

## **CHAPTER II**

### **THEORY OF WAVELET TRANSFORM**

#### **2.1 Introduction**

In this chapter, I will introduce the basics of wavelet transform, including general information and history. I will give the specific aspects of the wavelet theory and wavelet transform that will be used in the applications in Chapter III and Chapter IV.

##### **2.1.1 General information**

A wavelet is a wave-like oscillation so that the amplitude rises from zero and then falls to zero again. More visually, it could be observed as a brief oscillation from heart monitor or seismograph, with one major peak shown. Different wavelets are constructed with specific properties on purpose. This reason makes them useful tools for signal processing in different study areas. Wavelets can be convolved with any types of unknown signals to detect the information in the signals. This makes wavelets interesting and useful. Furthermore, since the wavelet has advantages over traditional Fourier method in analyzing non-stationary signals, the wavelet is widely applied in many scientific areas such as image compression, human vision, radar, earthquake prediction and geological structure construction.

### **2.1.2 History**

Wavelets are functions that match certain mathematical requirements in representing unknown signals. This idea started from early 1800's since Joseph Fourier discovered the Fourier method and used sine and cosine functions to represent other mathematical function. Because the Fourier transform has limitations for analyzing non-stationary and transient signals with different frequency contents, a new theory about wavelets was mentioned on Harr's work in the early 20<sup>th</sup> century. Then Zweig discovered the continuous wavelet transform in 1975. Gouplilaud, Grossmann and Morlet gave the CWT formula in 1982, followed by Jan-Olov Strömberg's early work on discrete wavelets in 1983. Thereafter, many works about wavelet started to give great impacts on different scientific fields, such as Daubechies's orthogonal wavelets with compact support in 1988, Mallat's multiresolution framework in 1989, Nathalie Delprat's time-frequency interpretation of the CWT in 1991 and Newland's Harmonic wavelet transform in 1993. These theoretical papers on wavelet analysis made great contributions to different study areas and have motivated the diversity of wavelet analysis applications. Results and implementations of this technology have been published all around the world on different scientific disciplines and application fields.

### **2.1.3 Wavelet theory**

Wavelet theory is based on the uncertainty principle of Fourier analysis respective sampling theory. All wavelet transforms may be considered as a time-scale representation for unknown signals related to harmonic analysis.

The wavelet analysis procedure is to adopt a self-adjusted wavelet prototype function called mother wavelet to different scale levels. A self-adjusted wavelet called daughter wavelet will be generated by prototype wavelet from low scale value to high scale value. Then the different daughter wavelets will convolve with the unknown signal to detect the information of similar frequency hidden inside the signal, and extract the information corresponding to that event by returning a wavelet coefficient. As a result, the unknown signal function could be represented as a combination of wavelet function and coefficients. This concept is the core of many practical applications of wavelet theory.

Wavelet theory have advantages over traditional Fourier theory in representing functions that have discontinuities in frequency, and accurately deconstructing and reconstructing finite, non-periodic and/or non-stationary signals. Therefore, wavelet transform has become a very efficient tool for different study areas in recent years.

#### **2.1.4 The continuous wavelet transform**

There are two major types of wavelet Transform: continuous and discrete. Both Discrete Wavelets Transform (DWT) and Continuous Wavelet Transform (CWT) are continuous time transforms, and can be used to represent continuous time signals. The CWT will take every possible scales and positions, while the DWT only uses specific scales and positions. Continuous Wavelet Transform is a more powerful tool for analyzing damping frequency in non-stationary signals, and it is also very resistant to the



noise in signal waves. Therefore, I decide to use CWT as a tool for hydrocarbon detection in my research.

The theory of continuous wavelet transform is to build self-adjusted window  $\Psi_{a,b}(x)$  of wavelet by translating in position (b) or dilating in scale (a):

$$\Psi_{a,b}(x) = \frac{1}{\sqrt{a}} \Psi\left(\frac{x-b}{a}\right) dx \quad (2.1)$$

Then take inner product with  $f(x)$  to get  $W(a, b)$

$$W(a, b) = \langle f(x), \Psi_{a,b}(x) \rangle = \frac{1}{\sqrt{a}} \int_{-\infty}^{+\infty} f(x) \Psi^*\left(\frac{x-b}{a}\right) dx \quad (2.2)$$

The wavelet transform function is defined as the following:

$$W(a, b) = \frac{1}{\sqrt{a}} \int_{-\infty}^{+\infty} f(x) \Psi^*\left(\frac{x-b}{a}\right) dx \quad (2.3)$$

where  $\Psi^*(x)$  denotes the mother wavelet,  $a$  is the scale parameter and  $b$  is position parameter.  $W(a, b)$  is called the coefficient of wavelet transform.

There are several properties for the wavelet transform shown as below:

1. The CWT is a linear transformation

$$af_x(x) + bf_y(x) \Leftrightarrow aW_x(a, b) + bW_y(a, b) \quad (2.4)$$

2. The CWT is covariate under translation

$$f(x) \rightarrow f(x - u) \Leftrightarrow W(a, b) \rightarrow W(a, b - u) \quad (2.4)$$

3. The CWT is covariate under dilation

$$f(x) \rightarrow f(ux) \Leftrightarrow W(a, b) \rightarrow u^{1/2} W(ua, ub) \quad (2.5)$$

## 2.2 Prototype wavelets

In this section, I give the wavelets I will use as mother wavelets. I will apply these wavelets to seismic data and build the spectrogram to detect hydrocarbon zone.

### 2.2.1 Morlet wavelet

The Morlet wavelet, named after Jean Morlet, was originally formulated by Goupillaud, Grossmann and Morlet in 1984 (Goupillaud, Grossman and Morlet, 1984). Conceptually related to windowed-Fourier analysis, the Morlet wavelet is a locally periodic wave-train. It is obtained by taking a complex sine wave, and by localizing it with a Gaussian (bell-shaped) envelope. The wavelet defined by Morlet is

$$\psi(x) = e^{-x^2/2} \cos(2\pi f_c x) \quad (2.6)$$

And the wavelet plot is shown in Figure 2.1.

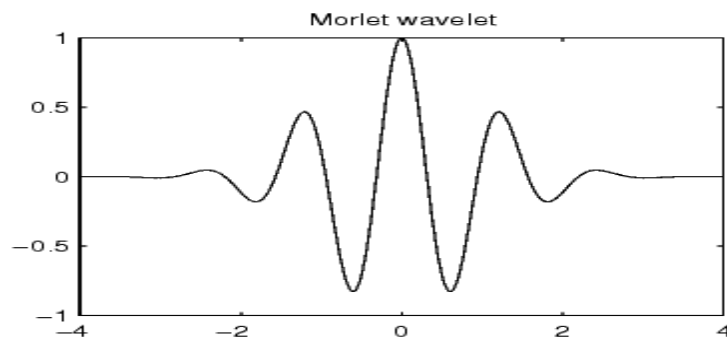


**Figure 2.1: Waveform of the Morlet wavelet**

### 2.2.2 Mexican hat (Ricker) wavelet

The Mexican hat wavelet is the negative normalized second derivative of a Gaussian function. It is usually known as the "Mexican hat" in the Americas. In technical filed this function is known as the Ricker wavelet, where it is frequently employed to construct seismic data. The Mexican hat defined by Murenzi is

$$\psi(x) = \frac{2}{\sqrt{3}} \pi^{-\frac{1}{4}} (1 - x^2) e^{-\frac{x^2}{2}} \quad (2.7)$$

And the wavelet plot is shown in Figure 2.2.

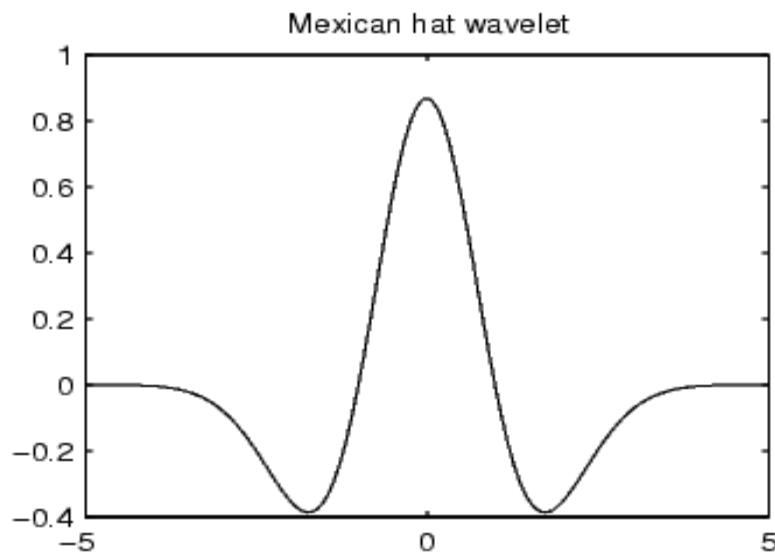


**Figure 2.2: Waveform of the Mexican hat wavelet**

### 2.3 Time-frequency analysis of wave signals

In my research, I will explore the potential of wavelet transforms for analyzing hydrocarbon information extracted from seismic data. The major scientific objective of this work is to examine the wavelet transform to identify important signatures across the time-frequency spectrogram (Liu and Miller, 1996). However, the direct result of wavelet transform is in time domain, so time varying frequencies need to be obtained during my research process. Therefore, this section aims at translating scales to frequencies so that the frequency content can be obtained locally associated with time.

The most efficient way is to associate a wavelet with a given central frequency  $F_c$ . As the wavelet transform process starts from numerical number “1” as a scale value, the maximum frequency will be equal to the central frequency divided by the sampling period of the unknown signal, which ties to the minimum scale value 1. As a result, each scale will be connected with an approximate frequency value based on the total scales. And when the wavelet is dilated by a factor  $a$ , this center frequency becomes  $F_c / a$ . If the underlying sampling period is  $\Delta$ , it is natural to tie the scale with the frequency numerically (Lang and Forinash, 1998):

$$F_a = \frac{F_c}{a \times \Delta} \quad (2.8)$$

where

- $a$  is the scale of wavelet transform;
- $\Delta$  is sampling period of the signal;
- $F_c$  is the center frequency of a given prototype wavelet in Hz;

- $F_a$  is the pseudo-frequency corresponding to the scale  $a$ , also in Hz.

To illustrate the behavior of this procedure, I will construct the following simple test. I will generate a sine function of a give frequency of 40Hz. For the sine function, I will try to detect the frequency of the sine function by a wavelet decomposition followed by a translation of scale to frequency. Figure 2.3 shows the sine wave used for the test.

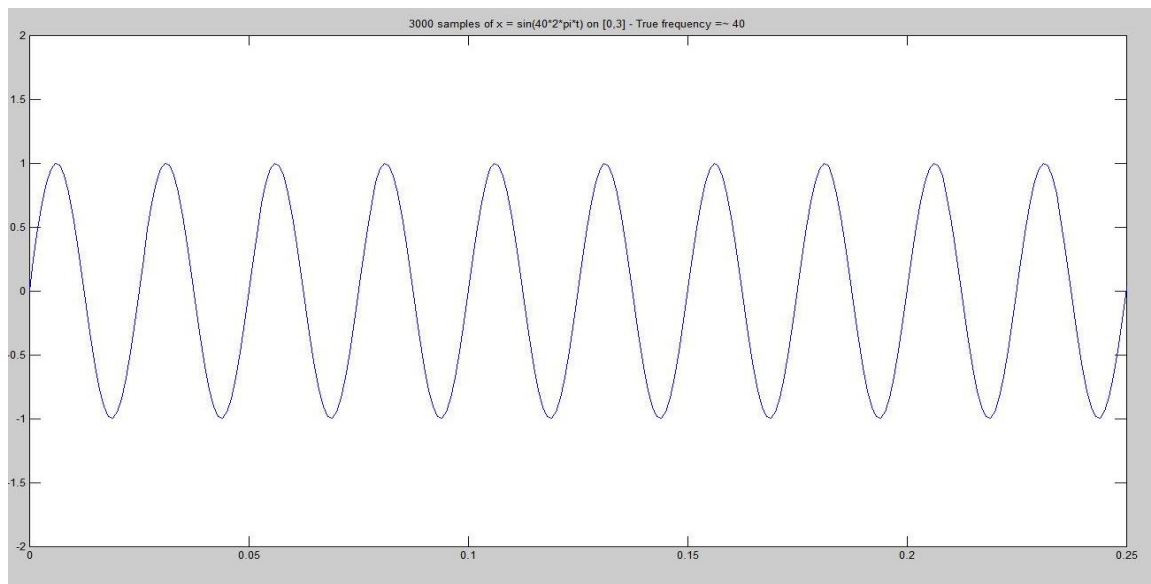


**Figure 2.3:** The sine waveform for  $x = \sin(40 \cdot 2 \cdot \pi \cdot t)$  on range of  $[0, 0.3]$

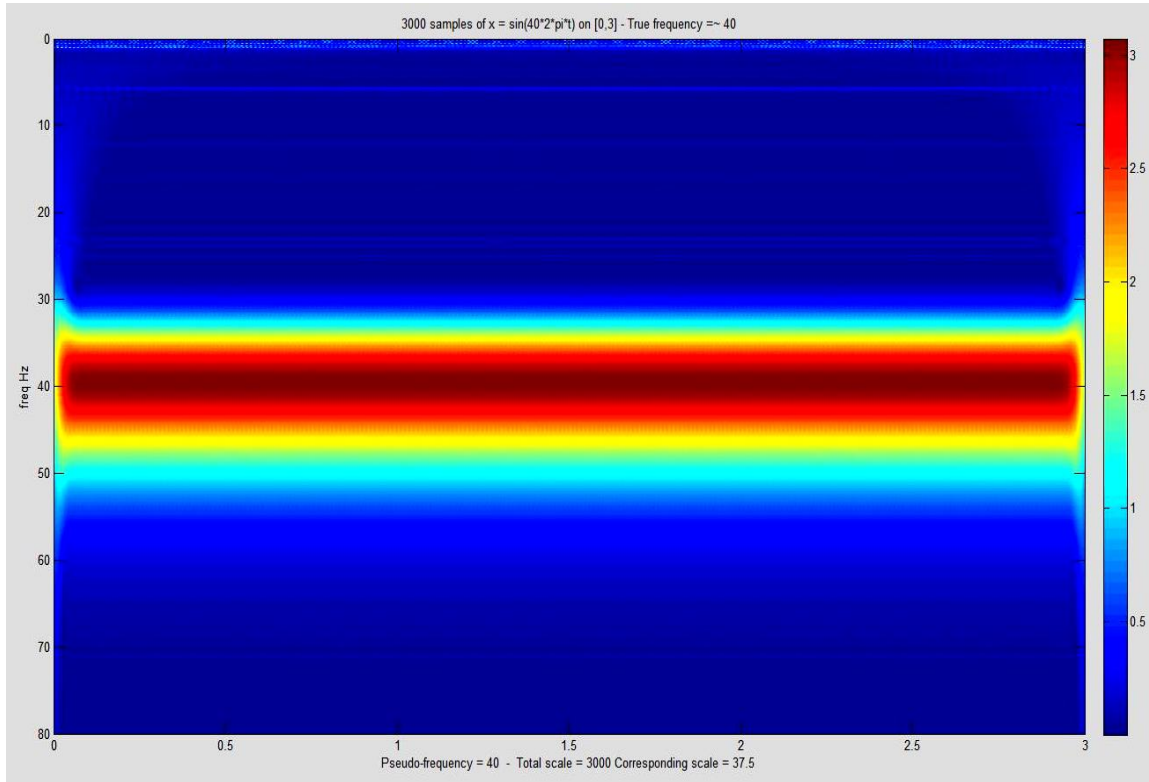


**Figure 2.4: The wavelet decomposition for the sine function  $x=\sin(40*2*\pi*t)$  shown in Figure 2.3**

As shown in Figure 2.4, the wavelet decomposition diagram captures the main frequency of the simple sine function. So this method of converting scale to frequency is a convenient and simple way of achieving time-frequency analysis for seismic wave decomposition.

Further test is done to interpret correctly the wavelet transform coefficients in the context of seismic attribute analysis. The equation of the testing wave is given as follows:

$$f(t) = \begin{cases} 0.2 * \sin (20 * 2\pi t) & 0 \leq t \leq 1.5 \\ 1 * \sin (20 * 2\pi t) & 1.5 < t \leq 2 \\ 0.5 * \sin (20 * 2\pi t) & 2 < t \leq 3 \end{cases} \quad (2.9)$$

The plot of the sine function with varying amplitude is shown in Figure 2.5. The sine function with a frequency of 20 Hz is used this time.

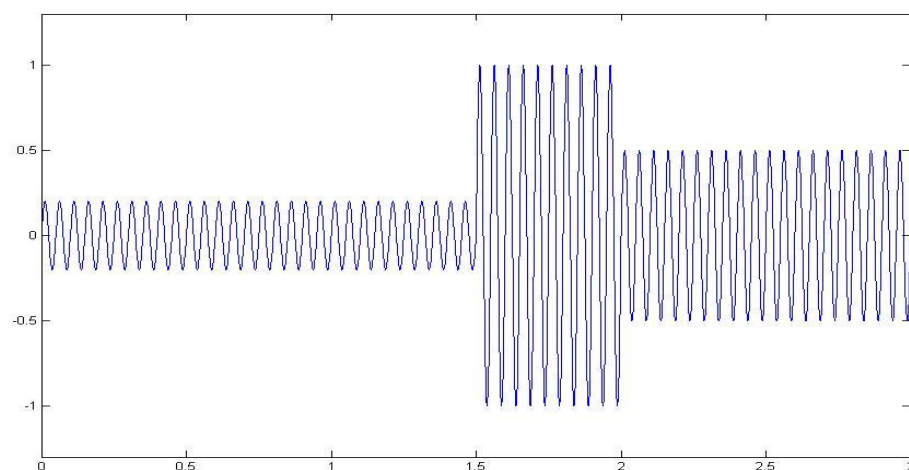


**Figure 2.5: The sine function with varying amplitude**

The spectrogram for this wave is shown in Figure 2.6. The highest energy area of the spectrogram is the portion of the wave train having the highest amplitude in the time domain. Therefore, I conclude that the wavelet transform detects the high energy portion of the wave train, showing as a high amplitude anomaly in the spectrogram at a given frequency and time.

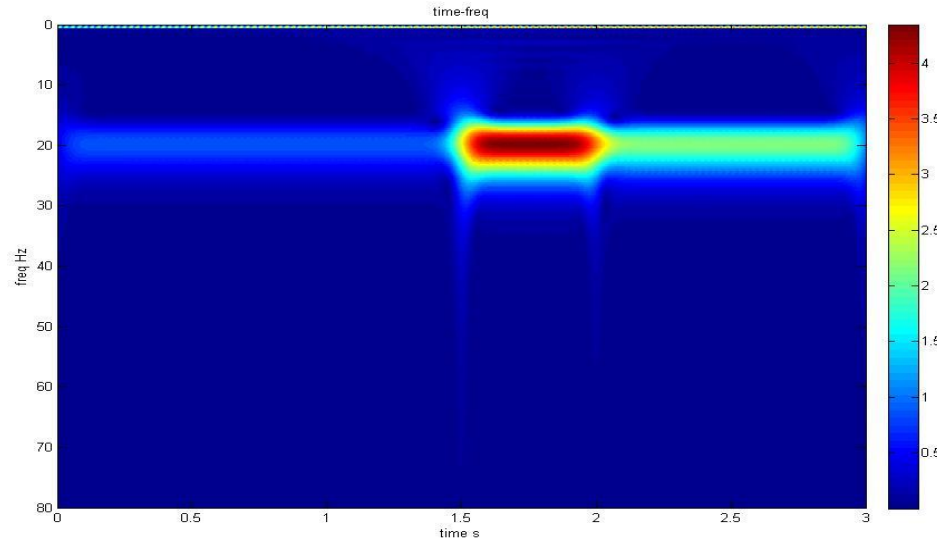


**Figure 2.6: The wavelet decomposition for the testing sine function with varying amplitude**

## 2.4 Comparison of different mother wavelets

The decomposition result of wavelet transform is not unique. By using different mother wavelets in the wavelet transform process, different spectrograms will be obtained. And the mother wavelets best for geophysical purpose will be used in my research. However, only one mother wavelet with the best performance will be selected for my further study. A real raw seismic trace from North Sea has been employed so that the difference of decomposition results can be observed realistically.



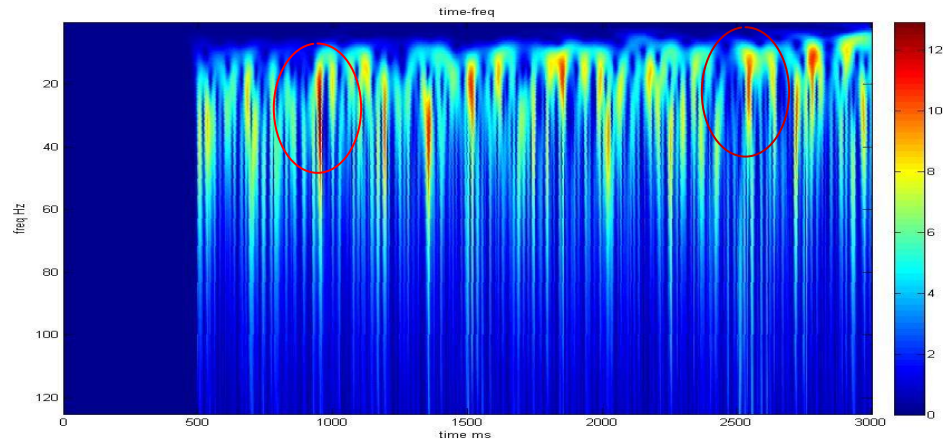


**Figure 2.7: The spectrogram of using Mexican hat wavelet**

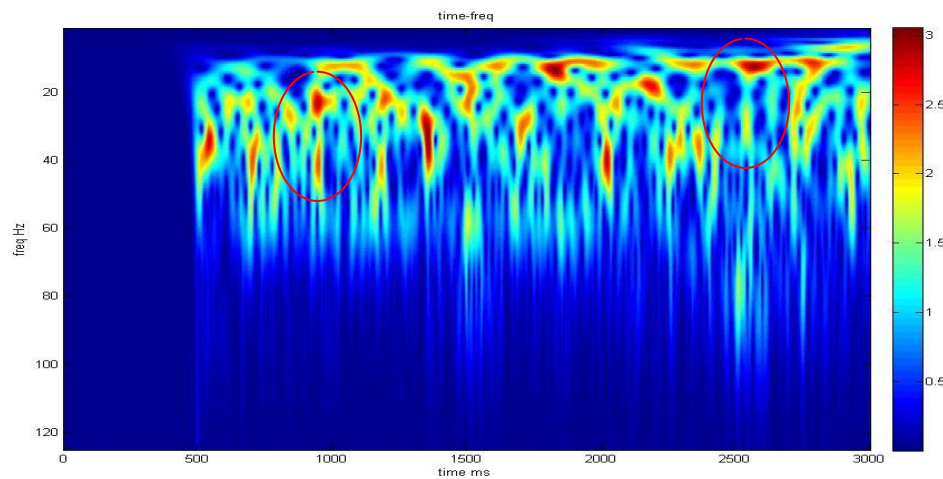


**Figure 2.8: The spectrogram of using Morlet wavelet**

The decomposition result of using Mexican hat wavelet is shown in Figure 2.7. And the decomposition result of using Morlet wavelet is shown in Figure 2.8. By comparing the two spectrograms, it is observed that the Mexican hat spectrogram has a better resolution in time domain but much lower resolution in frequency domain than the Morlet spectrogram. However, the major objective of this research is to detect high

energy zone in low frequency range possibly associated with hydrocarbons. If the frequency resolution is not sufficient to separate the wave information for different frequencies, valuable geological and fluid information will not be obtained by using wavelet transform. Therefore, the spectrogram with sufficient resolution for both time and frequency domain is the preferred result. Consequently, the Morlet wavelet that has the advantage in frequency resolution will be selected for further study.

## **2.5 Parameter selection for Morlet wavelet**

When wavelet transform is used, the different decomposition spectrograms can be obtained not only by applying different mother wavelet but also by using different parameters of the same mother wavelet (Ren, Weiland and Xiao, 2003). In Equation 2.1, the center frequency  $F_c$  of the Morlet wavelet can be changed for different purposes. However, the appropriate center frequency should be selected. Otherwise, the unexpected decomposition result without valuable information will be obtained. Figure 2.9 and Figure 2.10 illustrate the bad decomposition results for hydrocarbon detection purpose. They have either high resolution in time domain with extremely low resolution in frequency domain (Figure 2.9) or high resolution in frequency domain with very low resolution in time domain (Figure 2. 10).

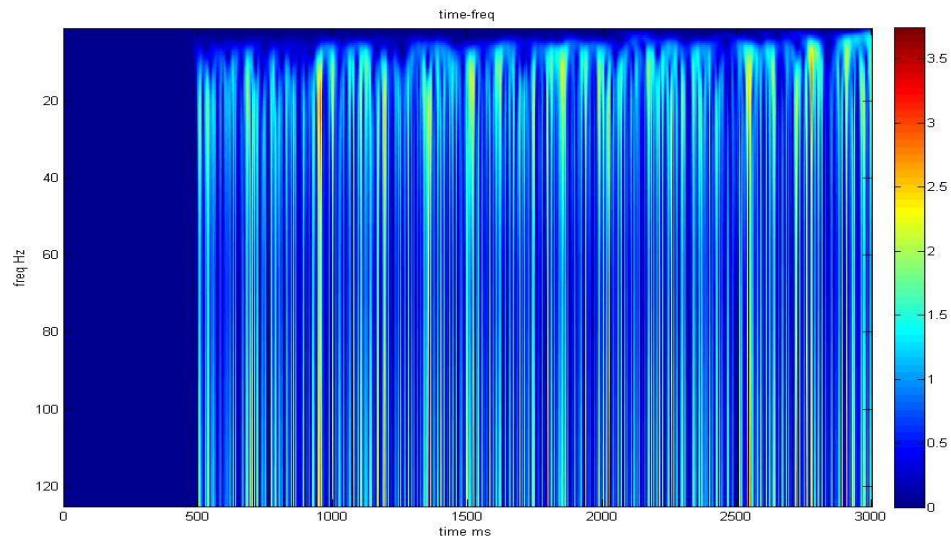


**Figure 2.9: The spectrogram with  $F_c=0.2$  Hz**

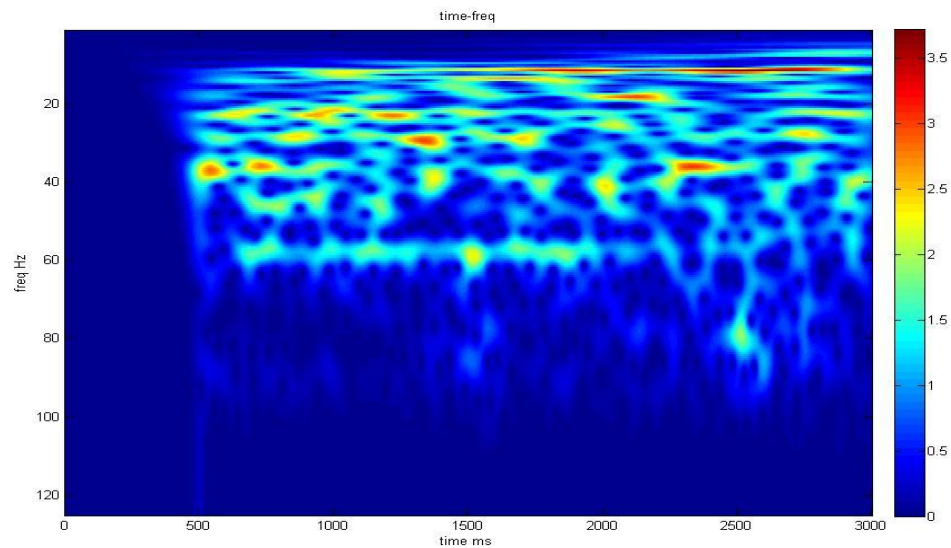


**Figure 2.10: The spectrogram with  $F_c=5$  Hz**

The Morlet decomposition result with center frequency value of 1.5 Hz is shown in Figure 2.11. Although the resolution in frequency domain is sufficient, the time

resolution in low frequency range still needs to be improved. Figure 2.12 shows the decomposition spectrogram with improved time resolution. And the center frequency of 1 Hz that I determined in Figure 2.12 will become my default mother wavelet frequency for further study in Chapter III and Chapter IV.

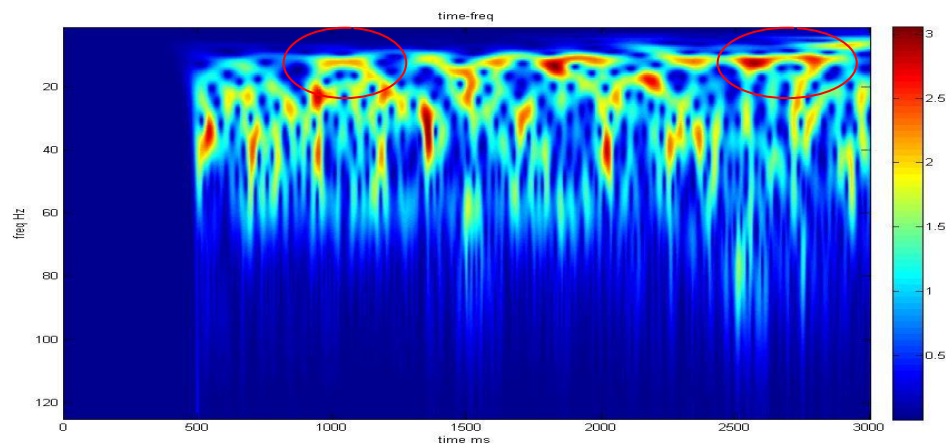


**Figure 2.11: The spectrogram with  $F_c=1.5$  Hz**

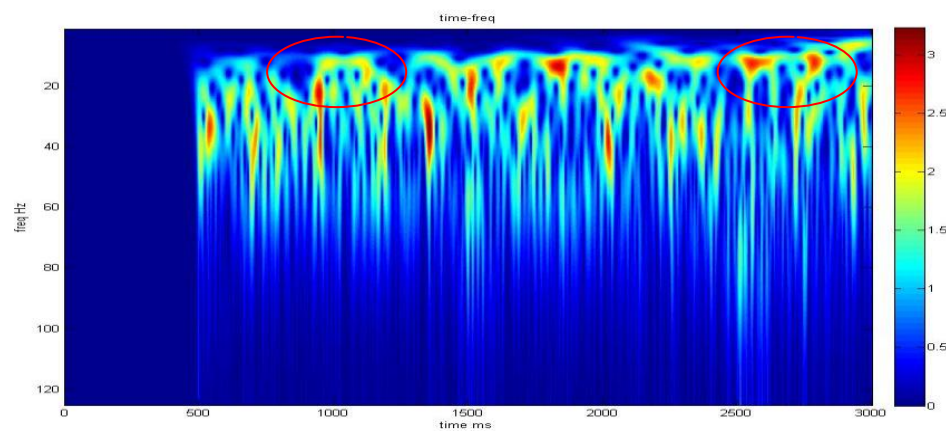


**Figure 2.12: The spectrogram with  $F_c=1$  Hz**

## 2.6 Conclusion

Wavelet is a useful tool to convolve with any types of unknown signals and detect the specific information hidden in the signals. Furthermore, the wavelet transform has the advantage over traditional Fourier transform and Short transform for analyzing non-stationary signals. The continuous wavelet transform will be applied to the seismic analysis due to its resistance to the noise in real seismic data. And conversion from scale to frequency makes the wavelet transform results be better interpreted for seismic analysis in oil and gas industry.

There are many prototype wavelets existing for different scientific purposes. Two conventional wavelets for geophysical purposes, Morlet and Mexican hat, are tested in my study. By comparing the decomposition spectrograms, the Morlet wavelet has been chosen for further study because the Morlet wavelet with appropriate center frequency can provide us with sufficient resolutions in both frequency and time, while Mexican hat wavelet can only provide high time resolution but very low frequency resolution when the default center frequency is used for the wavelet. Further study should also test different Ricker (Mexican hat) wavelets by varying its center frequency to check my conclusion, as the Ricker wavelet is important for seismic signal analysis and interpretation.

## **CHAPTER III**

### **SEISMIC ANALYSIS BY USING WAVELET TRANSFORM: THE CLASTIC RESERVOIR CASE IN THE NORTH SEA**

#### **3.1 Introduction**

After the wavelet transform is well understood in the context of seismic signal analysis and an optimal mother wavelet has been chosen, I apply the wavelet transform to my first real data set from a clastic reservoir in North Sea. The data was published by Exxon Mobile, and the location is in North Viking Graben area of the North Sea basin (Keys and Foster, 1998). The seismic data set are accompanied with complete petrophysical and well log data, providing solid background information about the hydrocarbon reservoir position and lithological composition. Furthermore, the geophysical and petrophysical data also provide me a way of verifying the hydrocarbon detection technique of using wavelet transform.

##### **3.1.1 Geological background of North Sea area**

The North Viking Graben area is located in the northern North Sea Basin as shown in Figure 3.1. This area was formed as a result of late Permian to Triassic rifting, and extensional sediment continued through the Jurassic into the early Cretaceous. Then by late Cretaceous, basin subsidence and filling became major movement in depositional process. The major gas reserves in North Viking Graben come from the Tertiary sandstones that trapped the dry gas and associated heavy oil.

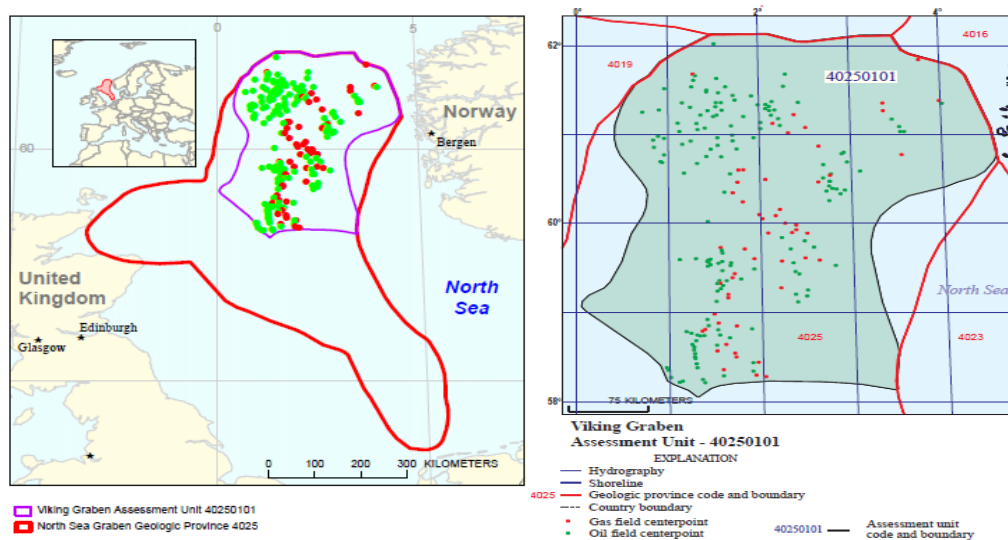


**Figure 3.1: Overview of North Sea area (From Viking Graben Assessment Unit 402501)**

It is an agreement that the major oil and gas accumulations in the northern North Sea were generated from certain fine-grained marine strata of late Jurassic and early Cretaceous. With 5 percent average organic carbon contents varying from 2 to 15, the source rock contains kerogen Type II that tends to produce oil and gas. (Goff, 1983)

The major reservoirs in the North Viking Graben are Jurassic age clastic sediments. And the depositional environment types include fluvial, deltaic and shallow marine. The reservoir intervals are formed by coarse clastic sedimentary rock and separated by deep water shale. These reservoirs are hundreds of meters thick, with porosity in excess of 30 percent. The Paleogene submarine fan and channel sandstones are also significant reservoirs in this area.

In the North Viking Graben area, hydrocarbon traps are usually fault bounded structures. Some traps are associated with stratigraphic truncation of the base



cretaceous unconformity (Pegrum and Spencer, 1991). The largest hydrocarbon accumulations were caused by rifting formed faults. These faults stratigraphically trapped hydrocarbons in submarine channel. Furthermore, Tertiary fine –grained marine mudstones deeply bury most traps in the Viking Graben and provide an effective regional seal.

### 3.1.2 Testing well information

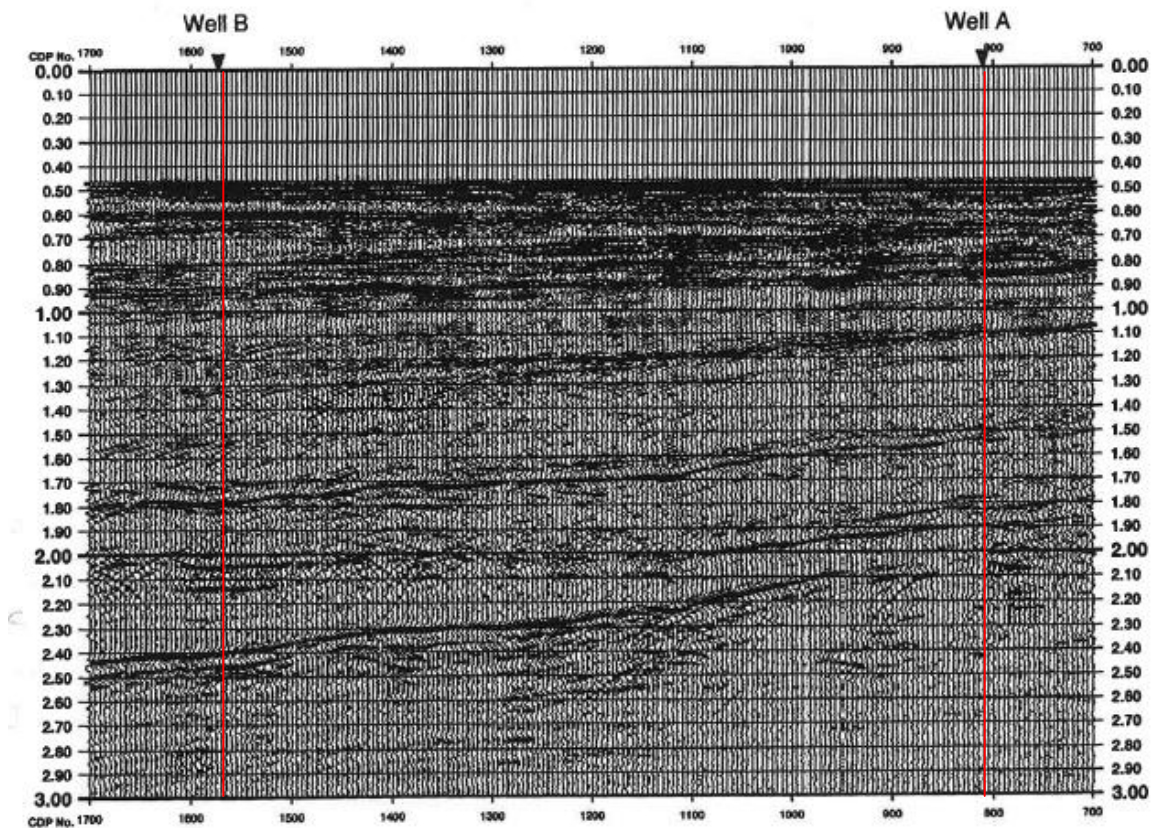


**Figure 3.2: Seismic line after stack for North Sea data (From *Comparison of Seismic Inversion Methods on a Single Real Data Set*)**



Figure 3.2 shows one seismic line of the North Viking Graben collected for AVO study. The two wells I use to verify my wavelet transform results are Well-A and Well-B, which intersect the seismic line as indicated in the figure. Well-A intersects the seismic line at shot point 440 and Well-B intersects the seismic line at shot point 822.

Based on the references published by Exxon Mobile (Keys and Foster, 1998), a significant unconformity where the first reservoir is located occurs at the base of the cretaceous. The two-way travel time of this unconformity appears at approximately 1.97s in Well-A and 2.46s in Well-B.

The second reservoir appears at approximately 1.6s in Well-A and 1.9s two way travel time in Well-B. This reservoir is the Paleocene deep water clastic reservoir which is deposited in a slope environment. This regressive pulse associated reservoir is undisturbed by the rift tectonics and dips gently into the basin. And hydrocarbon traps of this type reservoir are depositional mounded structures or stratigraphic pinchouts.

### **3. 2 Seismic data analysis by using wavelet transform**

In this section, the wavelet transform will be applied to the seismic data, both for synthetic and real seismic traces in order to match the hydrocarbon appearance provided by the petrophysical data.

#### **3.2.1 Wavelet analysis for synthetic trace at well location**

First of all, I will test the method at well locations by using the provided lithology information, rock properties and locations of the hydrocarbon zones. A

synthetic seismic trace at the well location will be constructed to link the well log data to real seismic data as shown in Figure 3.3. Only primary seismic waves will be generated in synthetic seismic trace with no multiples. The wavelet transform result will be applied to the synthetic trace to verify its validity.

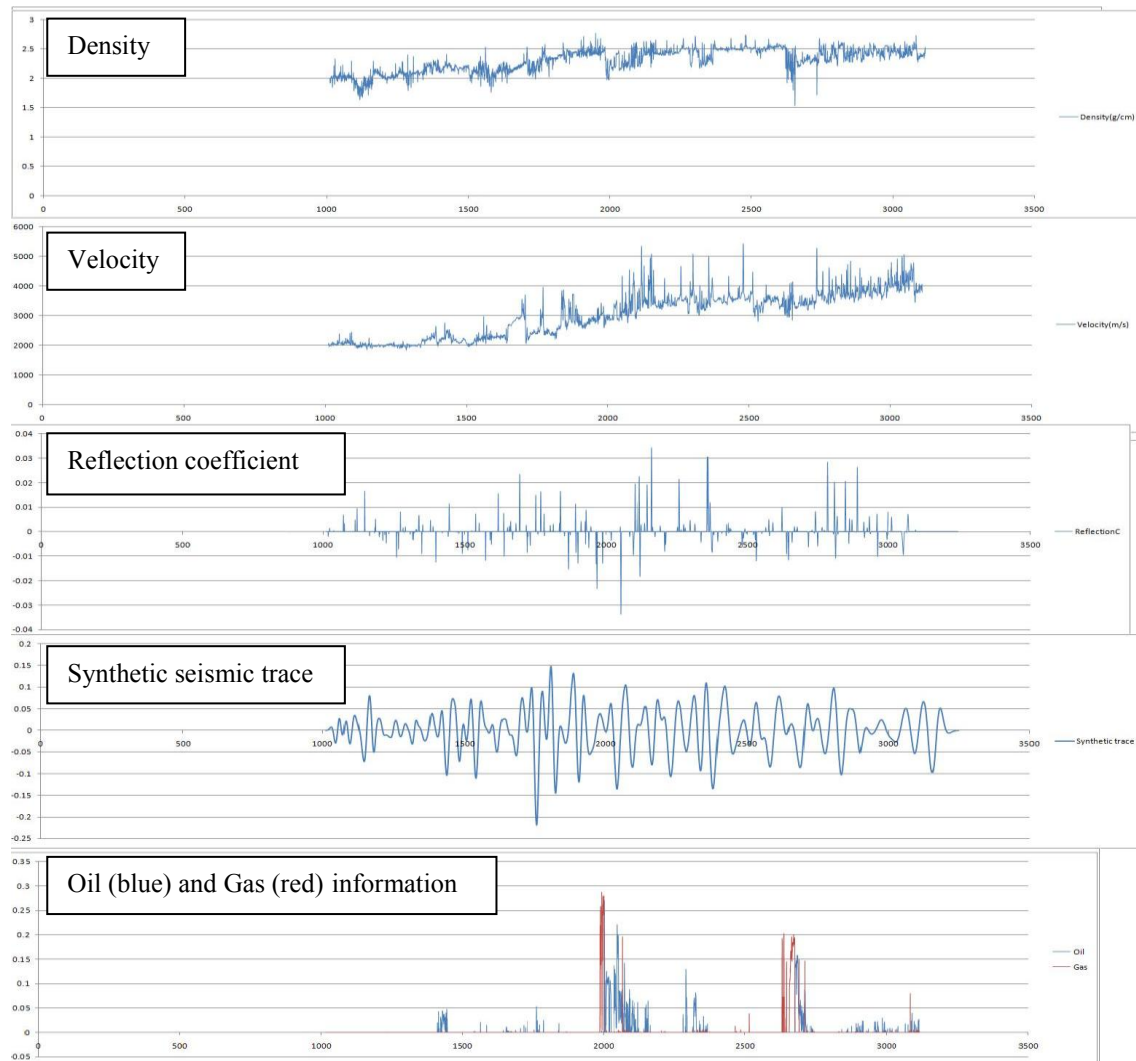


**Figure 3.3: Synthetic data trace construction shown in depth**

Based on the fact that the log data has a sampling interval much smaller than the vertical resolution of the seismic data, the desired result from log-based synthetics could give the signature of the two major reservoirs after the wavelet transform decomposition. A 1-D synthetic seismic trace will be generated from given density and velocity log data at Well-A location, by convolving calculated reflection coefficient with a Ricker wavelet. Then I will try to tie the synthetic seismic trace with the real seismic trace, because the real seismic reflection data is initially only available in the time domain.

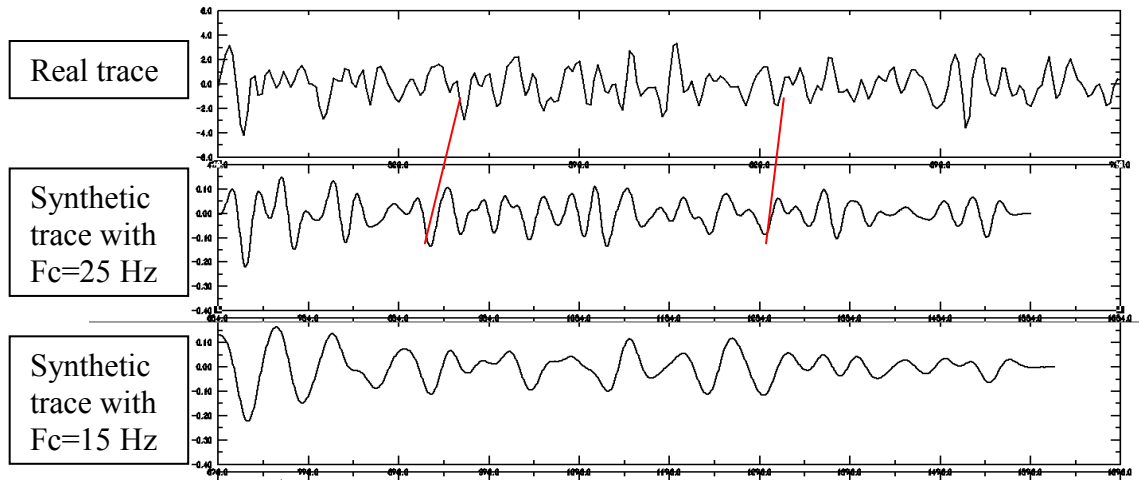


**Figure 3.4: Center frequency selection and well seismic tie**

During the process of synthetic seismic trace construction, special attention should be paid to the frequency content so that the synthetic trace could match the real seismic trace. As shown in Figure 3.4, the synthetic trace with 25Hz center frequency matches the real seismic data trace better than that with 15 Hz wavelet. Therefore, the

synthetic seismic trace with 25 Hz center frequency will be used for my wavelet analysis process.

Because this synthetic seismic trace is generated from compressional velocity and density at Well-A location, the predicted signature for the wavelet decomposition will be high energy spots where the  $V_p$  and density change abruptly. I did not consider attenuation when building the synthetic seismic trace. Hence, no frequency attenuation will be observed in the spectrogram (Singleton, Taner and Treitel, 2006). Based on the information provided in the petrophysical and log data, there are two major hydrocarbon zones. As a result, there should be also two high energy signatures showing on the spectrogram.

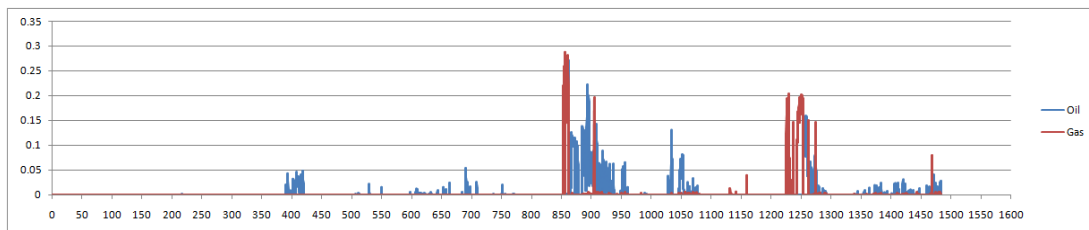


**Figure 3.5: The oil & gas information at Well-A location. Y-axis represents volume percentage and x-axis represents time in ms**

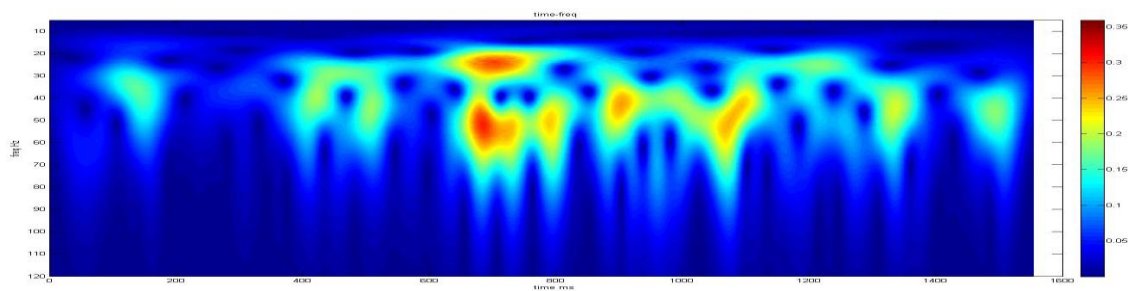


**Figure 3.6: Spectrogram for the synthetic seismic trace**

The well log data start at 1000 meters under the sea level. However I will use 0 ms as the relative starting time when I convert depth to time. Figure 3.5 provides the hydrocarbon information while Figure 3.6 shows the spectrogram for synthetic seismic data at Well-A location. And the signature fits the hydrocarbon information.

### 3.2.2 Wavelet analysis for real seismic data trace at well location

After obtaining the desired result from building the spectrogram for the synthetic seismic trace, I could use the same techniques to construct the spectrogram for real seismic trace. However, there may be some factors that will influence the final result of the wavelet decomposition of real seismic data. This real seismic data set has only a sampling interval of 4ms which is low using the current standard. In addition, the seismic data provided by Exxon Mobile is pre-stack raw seismic shot gathers without any data processing so that they contain multiples and noise. Therefore, observation of the major signature of high energy zones may be comprised. As the real seismic data is used this time, the frequency attenuation could also be observed in the spectrogram.

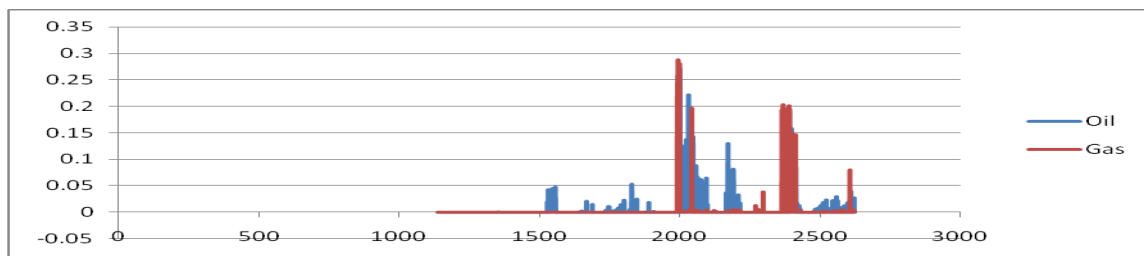


**Figure 3.7: The oil & gas diagram in real time at Well-A location. Y-axis represents volume percentage and x-axis represents time in ms**

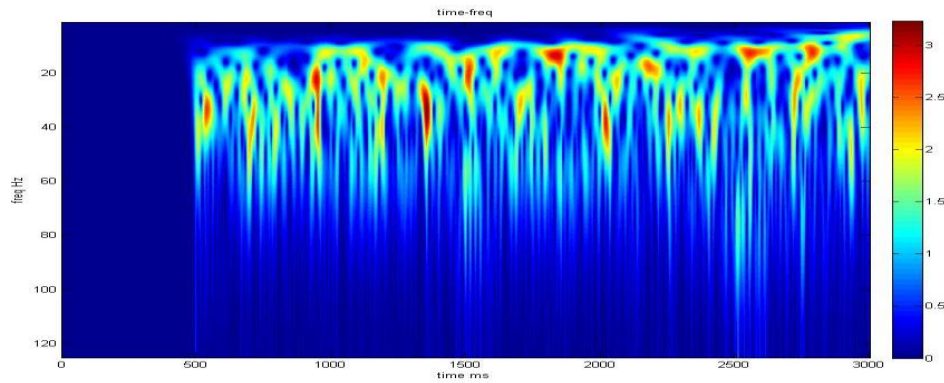


**Figure 3.8: Spectrogram for real seismic trace at Well-A location**

The hydrocarbon information in real time is provided in Figure 3.7, while the spectrogram in Figure 3.8 shows the wavelet decomposition result. The major frequency change appears approximately at 1.5 s which is the location of the first reservoir. There are also two major signatures of the high energy zones observed approximately at 1.8 s and 2.5 s. The frequency that could catch the high energy zone is around 15 Hz to 20 Hz, while 40Hz-50Hz frequency range could be used for shallow layer detection.

In order to validate the information obtained from wavelet analysis for Well-A, the spectrogram for Well-B is also obtained. Based on the hydrocarbon information shown in Figure 3.9, there will be one major frequency attenuation and three major high energy zones observed in the wavelet analysis spectrogram. Furthermore, the major frequency attenuation will appear at the major unconformity above the first reservoir at approximately 2 seconds which is the first reservoir location from Exxon Mobile's interpretation.

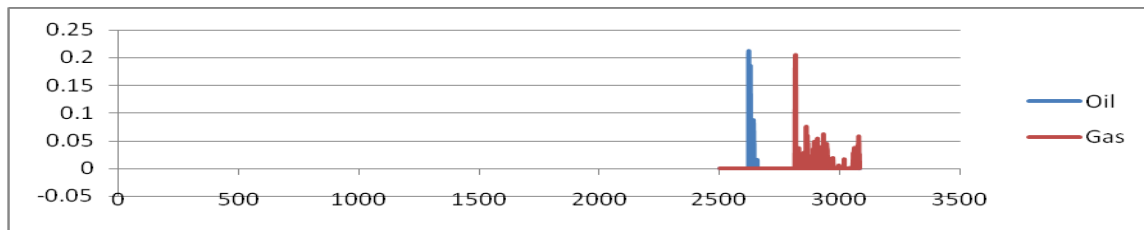


**Figure 3.9: The oil & gas information at Well-B location. Y-axis represents volume percentage and x-axis represents time in ms**

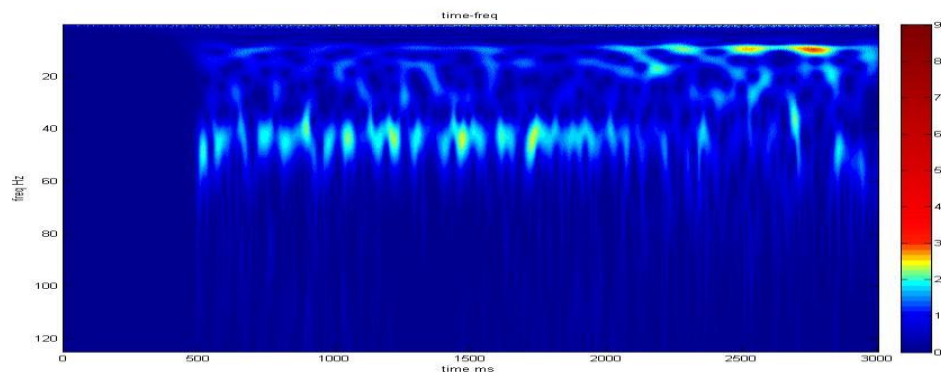


**Figure 3.10: Spectrogram for real seismic trace at Well-B location**

The spectrogram in Figure 3.10 shows the wavelet decomposition result at Well-B location. The major frequency attenuation appears approximately at about 2 seconds which is the location of the unconformity above the first reservoir based on Exxon Mobile's interpretation. Two major signatures of high energy zone can be observed approximately at 2.5 seconds and 2.7 seconds. The frequency that could catch the high energy zone is around 15 Hz, while 40Hz-50Hz frequency range could also be used for shallow layer detection.

The information obtained from these two spectrograms approximately match both predictions and petrophysical and log data, therefore, further steps could be taken with this North Sea raw seismic data for the wave decomposition analysis.

### 3.2. 3 Seismic section generated by using wavelet transform

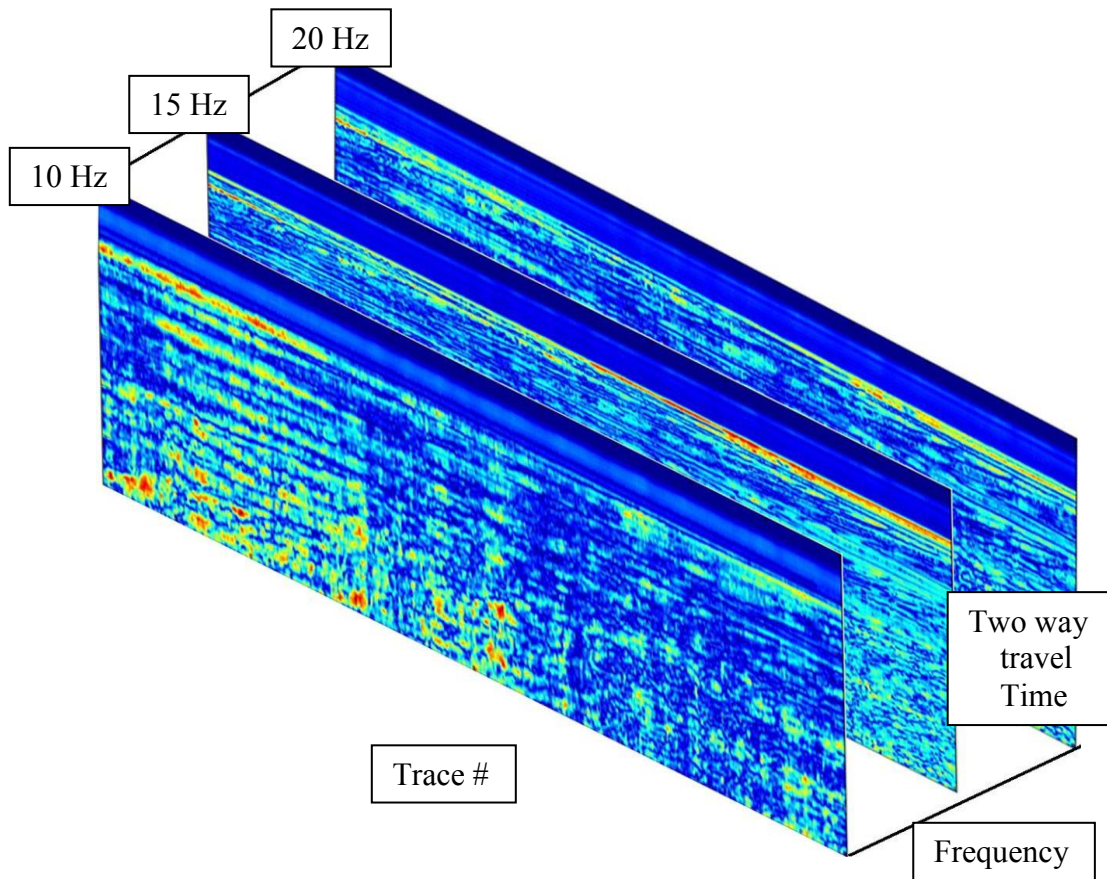
After obtaining the spectrograms for both Well-A and Well-B, I use the information for further steps and process the wavelet transform for the entire 2-D seismic data. A cross section spectrogram will be constructed. High energy zone will be observed in low frequency range around 10Hz to 20Hz. Shallow beds information also could be obtained by constructing the spectrogram at 45 Hz to 50 Hz. Then I will use the energy balancing equation to process the spectrogram in order to provide a better view. The energy balancing equation is show as following:

$$A_{\text{new}} = A_{\text{old}} \times \frac{K}{K1} \quad (3.1)$$

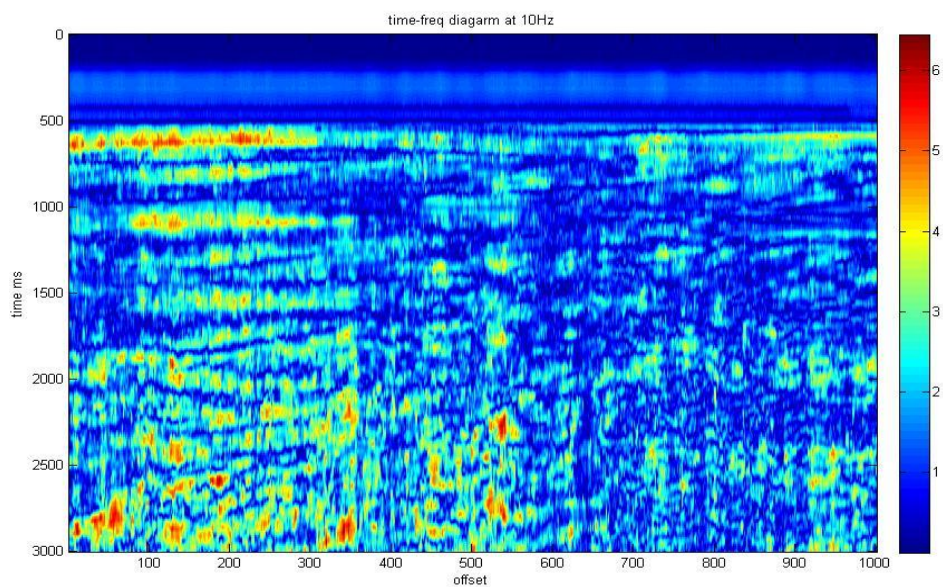
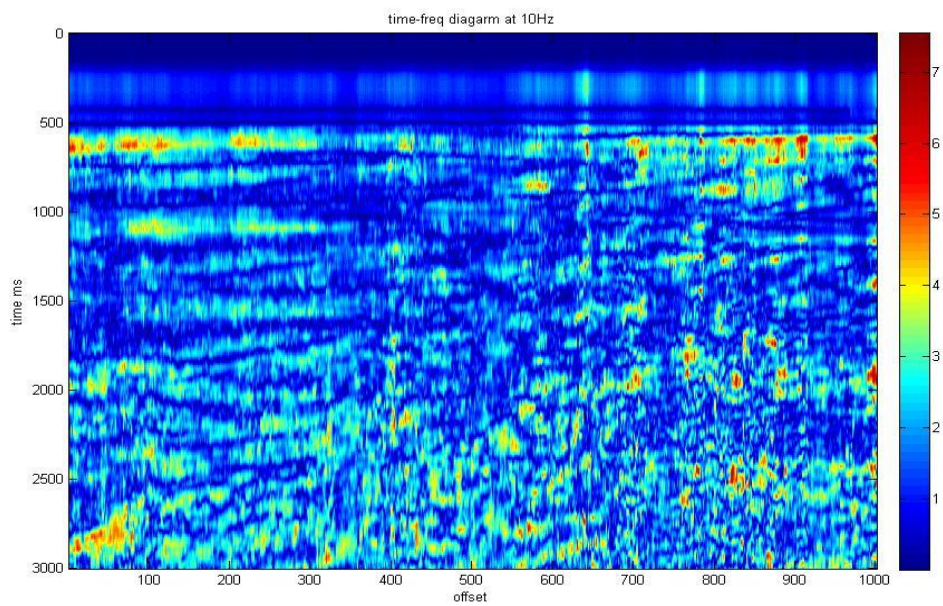
where

- $A_{\text{new}}$  is the balanced value of one data unit;
- $A_{\text{old}}$  is unbalanced value of one data unit;
- $K$  is the average value of the entire spectrogram;
- $K1$  is the average value of the column which A belongs to.





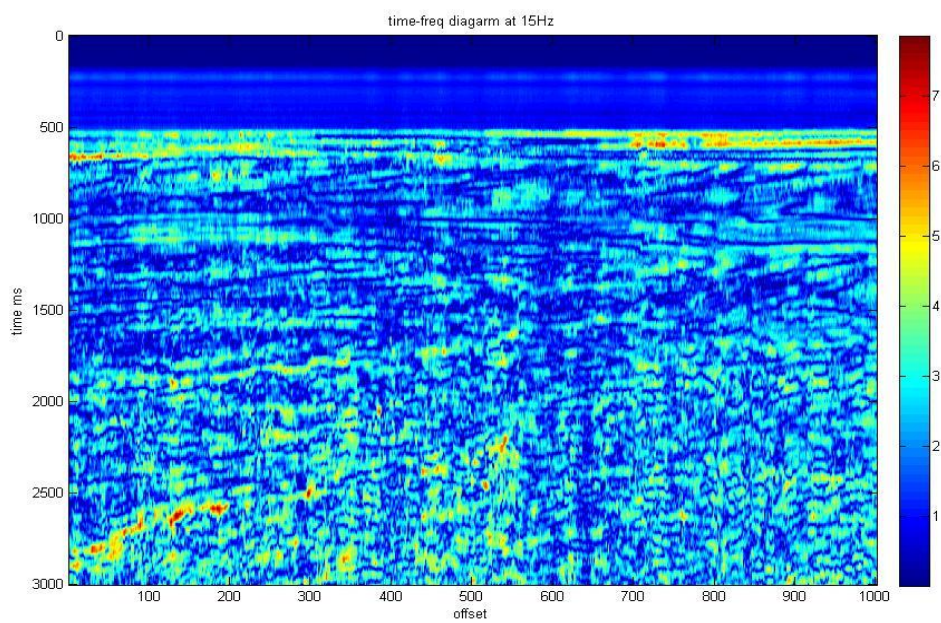
**Figure 3.11: The 3-D Diagram of decomposed cross section**

**(a)****(b)**

**Figure 3.12: Cross section spectrogram at 10Hz. (a) amplitude unbalanced diagram  
(b) amplitude balanced diagram**



(a)



(b)

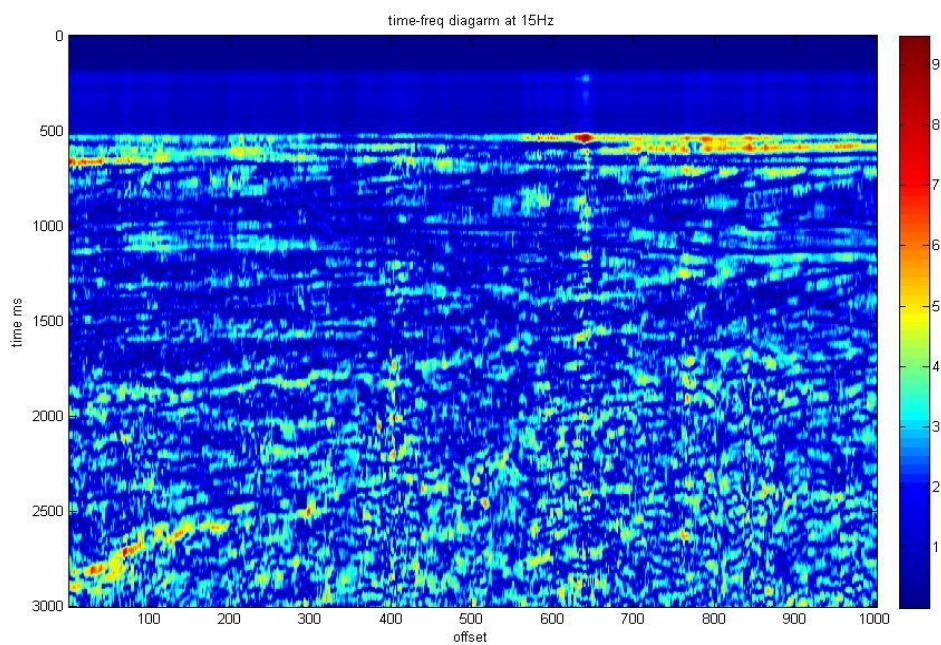


**Figure 3.13: Cross section spectrogram at 15Hz. (a) amplitude unbalanced diagram  
(b) amplitude balanced diagram**

Figure 3.12 and Figure 3.13 show the cross sections obtained by using wavelet transform. Figure 3.12 represents 10Hz spectrogram, while Figure 3.13 represents the cross section spectrogram with 15Hz. These two spectrograms with low frequency indicate the high energy zones in this area. As the frequency increases, the high energy zones disappear and the thin beds appear on the cross section spectrogram, which is shown in Figure 3.14.

(a)

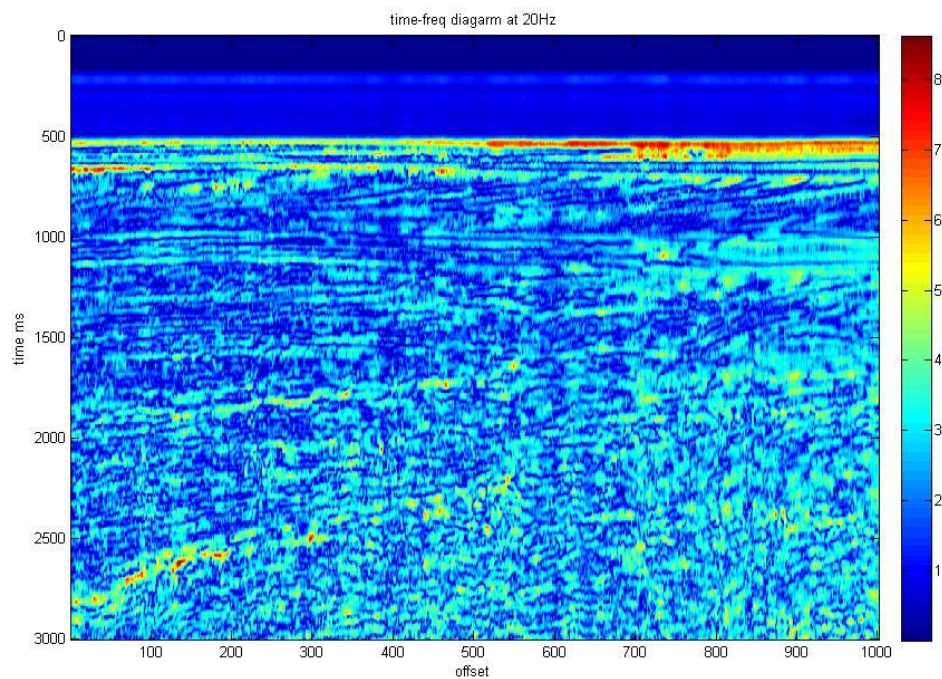


**Figure 3.14: Cross section spectrogram at 20Hz. (a) amplitude unbalanced diagram  
(b) amplitude balanced diagram**



(b)

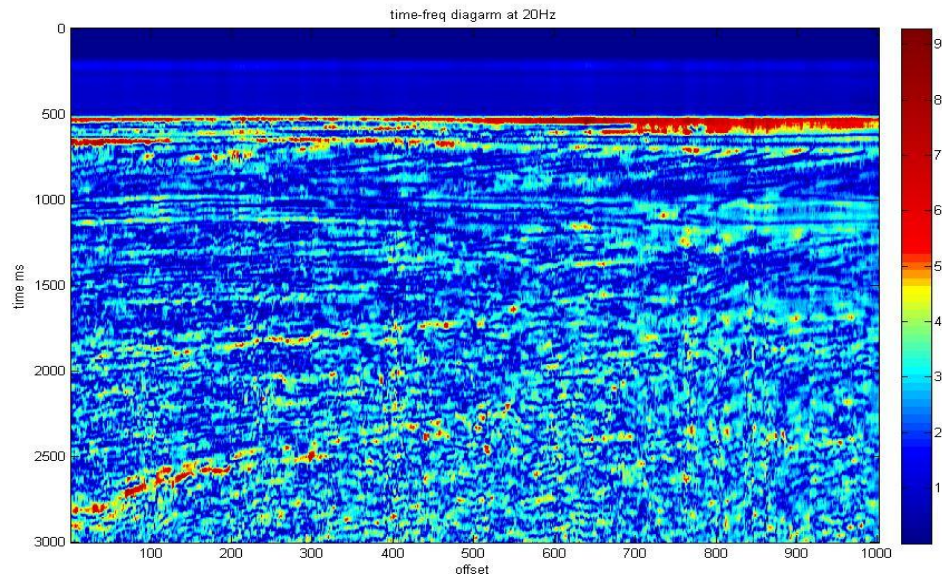


**Figure 3.14 continued: Cross section spectrogram at 20Hz. (a) amplitude unbalanced diagram (b) amplitude balanced diagram**

(a)

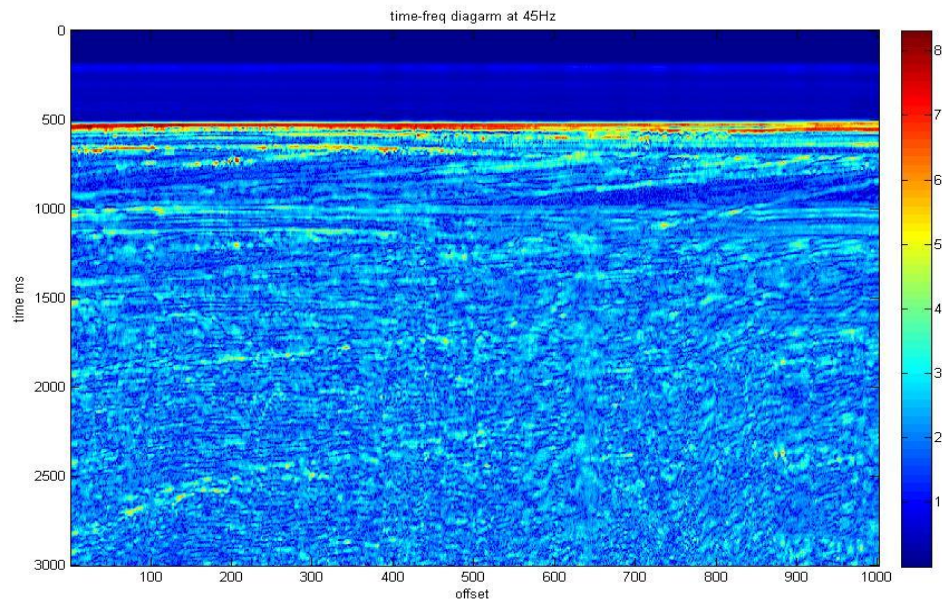


**Figure 3.15: Cross section spectrogram at 45Hz. (a) amplitude unbalanced diagram (b) amplitude balanced diagram**

(b)

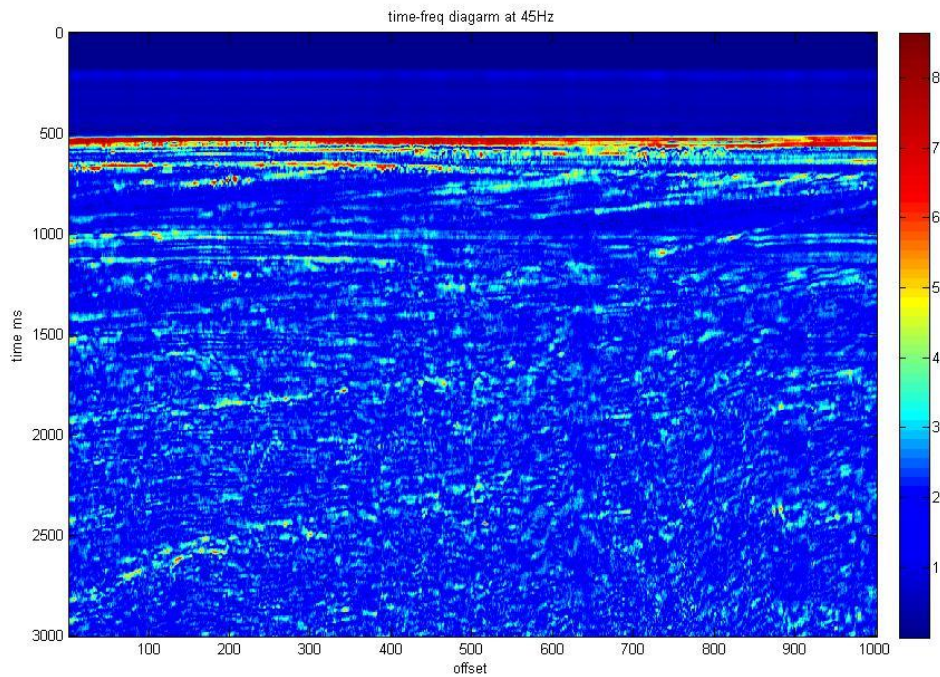


**Figure 3.15 continued: Cross section spectrogram at 45Hz. (a) amplitude unbalanced diagram (b) amplitude balanced diagram**

The high frequency cross section spectrogram is constructed for shallow beds identification. As shown in Figure 3.15, the high energy zones disappear in this spectrogram and have a very high resolution in the time domain so that thin beds can be separated.

### 3.3 Conclusion

My first seismic analysis using wavelet transform is done for clastic reservoir in the North Viking Graben area located in the North Sea basin. Compared with the know major reservoirs drilled through at well locations, results shown in the decomposition

spectrograms obtained using wavelet transform technique give high energy amplitudes at lower frequencies than both above and below the reservoir zones. Nevertheless, the temporal resolution is rather low.

Because this seismic data set is a raw seismic data set, result from the one-fold seismic section has been affected by the multiples and noise. However, high energy zones can still be observed at lower frequency from the cross section spectrogram. In particular, results at the Well-B location agree with the known hydrocarbon occurrences provided by the well logs. This demonstrates that the wavelet analysis could be a useful tool to assist geological interpretation in clastic reservoirs.

## **CHAPTER IV**

### **APPLICATION ON ORDOVICIAN FOSSIL KARST**

### **FRACTURE CAVITY RESERVOIR**

#### **4.1 Introduction**

In this chapter, I will apply wavelet transform to seismic analysis for hydrocarbon prediction in an Ordovician paleo-karst reservoir. Deeply-buried karst reservoirs have recently become active areas of exploration. However, because of their great depth, seismic reflection signals are usually weak and signal/noise (S/N) ratio is low. In addition, karst reservoirs exhibit great heterogeneity in size, shape and connectivity. Above all, there hardly exist any core data and well logs available within the reservoirs. Karst reservoir prediction is very difficult subject. I will use the wavelet analysis technique to investigate its feasibility for hydrocarbon prediction in karst reservoirs.

##### **4.1.1 Geological background**

The Ordovician carbonate reservoirs in the studied basin can be grouped into four types, which are paleo-weathered-crust reservoirs, reef reservoirs, buried karst reservoirs and dolomite reservoirs. Two separate proprietary seismic datasets will be used in this analysis, although the detailed geological, petrophysical and geophysical information associated with the data sets is not available to this study.



The carbonate rocks of the Ordovician age were subjected to weathering for a long time, forming karst systems that became good reservoirs to trap hydrocarbons. Late structural movements in the region caused well-developed carbonate fracture systems. Consequently, the storage capacity of the reservoirs had been greatly improved, and a good environment for the development of secondary pore space had been created. Therefore, the karst carbonate reservoir is an important target for hydrocarbon exploration. A typical structure of Ordovician Karst fracture-cavern reservoir is shown in Figure 4.1. It might provide an analog for the karst fracture-cavern reservoir that exists in my studied area.

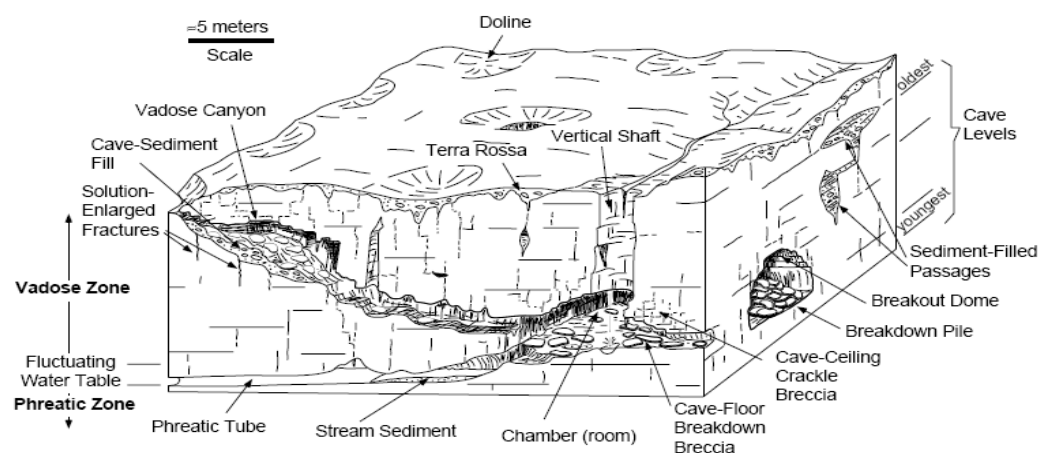


**Figure 4.1: Basic structure of Ordovician karst fracture-cavern reservoir (Modified from Loucks and Handford, 1992)**

#### **4.1.2 Basic concept of using wavelet analysis for the karst reservoir**

Although the karst carbonate reservoirs could be potentially a major target for hydrocarbon exploration, there are many factors causing trouble for oil and gas detection

in these reservoirs. For the studied reservoir, the deeply buried target layers locate greater than 5000 meters resulting in weak seismic reflection signal and low signal/noise ratio. Secondly, dissolution pores, cavities, structural fractures cause the great heterogeneity in terms of carbonate reservoir type variation. Thirdly, the distribution of oil, gas and water in the reservoir is complicated. All of these factors bring great difficulty to hydrocarbon prediction(Yang, Xiao and Peng, 2009).

The generic analysis of the deep-buried reservoir of the Ordovician carbonate rocks is also difficult. The carbonate rocks are deeply buried from about 4000 to 7000 meters in this basin. The reservoir properties formed in this depositional environment have been strongly modified during the burial process. The different burial depth in different areas results in diversities of burial temperature, pressure, underground water hydrochemistry and various physicochemical changes, which impact on the reservoir properties. Therefore, the wavelet analysis could play more important role for hydrocarbon detection in this type of reservoirs.

In this basin, Ordovician fracture cavity reservoirs are the major type of producing formations. The seismic response of the reservoir changes depending on the thickness of the fracture cavity reservoir. If the fracture-cavity reservoir beds are less than 2- ms in two-way travel-time below the top Ordovician, the seismic reflection will become weak or absent. The effect on top Ordovician reflection becomes weaker with deeper burial of fracture cavity reservoir beds, but the deep fracture cavity reservoir beds cause stronger reflection in the interior of the Ordovician. Based on understanding of

these basic reflection characteristics, the wavelet decomposition technique can be used to detect oil zone in Ordovician fracture cavity carbonate reservoirs.

## **4.2. Wavelet decomposition analysis for karst carbonate reservoir**

In this section, the wavelet transform method will be applied for karst fracture cavity reservoir. Wavelet transform will be done on one seismic trace first for parameter analysis. Then Xline cross section spectrogram, inline cross section spectrogram and time slice spectrogram will be constructed to illustrate the usage of this technique.

### **4.2.1 Trace analysis using wavelet transform**

Before applying wavelet decomposition analysis techniques to the seismic cross section, a real seismic trace at well locations should be analyzed first to check the validity. Based on the information obtained from the previous chapter, there will be frequency attenuation from top to the bottom as the depth increases. High energy spots appearing at low frequency may indicate hydrocarbon zones. The seismic data traces used in this section are processed post-stack seismic data traces. Therefore, the seismic data traces have a higher S/N ratio and could potentially provide a better decomposition result than the data in the previous chapter. Three testing wells will be used for trace analysis. The information for these three testing wells is shown in Figure 4.2. Testing Well-1 has oil production at approximately 3.41 second, while testing Well-3 has a water zone at 3.42 second. There is no cave found in testing Well-2 location at approximately 3.38 second, which is under the top of Ordovician fracture cavity reservoir.

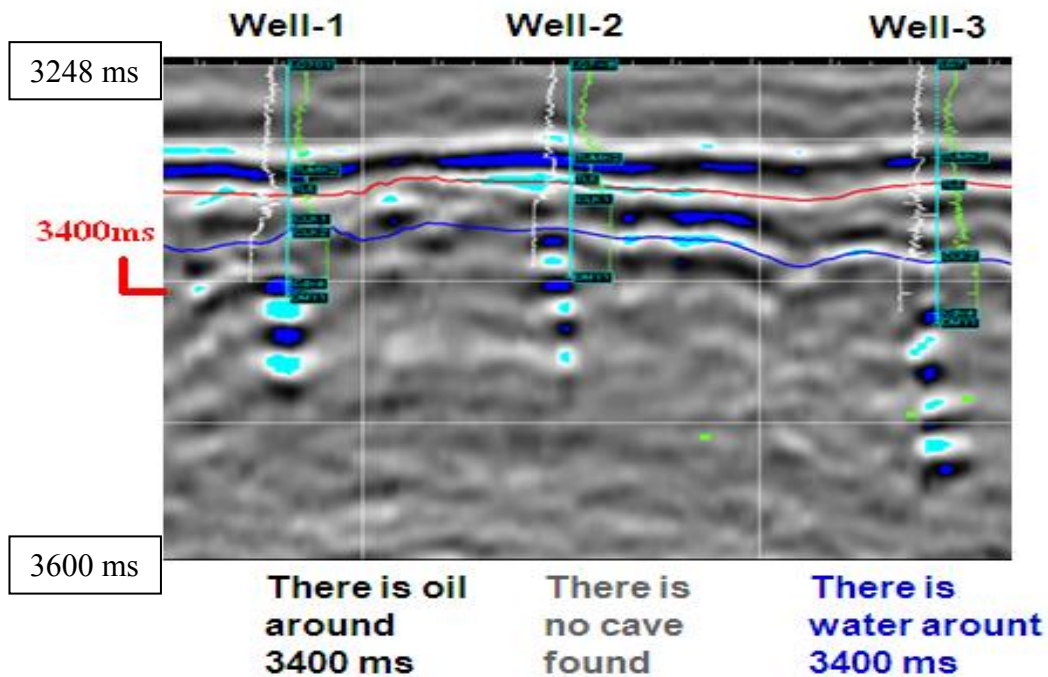


**Figure 4.2: Cross section for Ordovician fracture cavity reservoir with testing well information**

From the seismic cross section in Figure 4.2, it is observed that each testing well shows high amplitude indicating a cave except Well-2. However, only Well-1 has oil production while other two wells miss the hydrocarbon zone. Based on the geological information provided in the document, there is also a significant lithology change from Triassic shale to Ordovician fracture cavity reservoir.

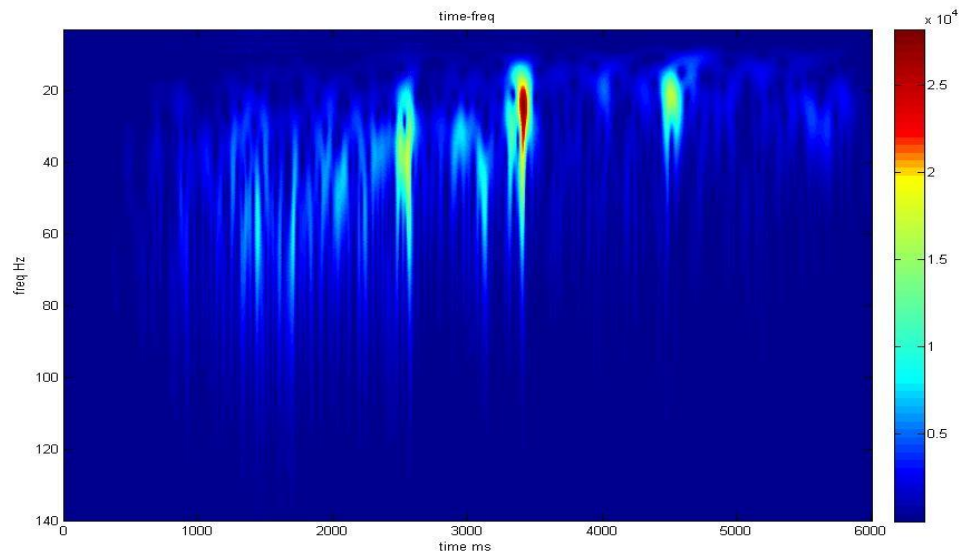


**Figure 4.3: Spectrogram for seismic trace at Well-1 location**

The spectrogram for seismic trace at Well-1 location is shown in Figure 4.3. A high energy zone appears at approximately 3.4 seconds with a relatively low frequency in this spectrogram, corresponding to the hydrocarbon occurrence. The stratigraphic information could also be observed with a relatively high frequency (above 40 Hz) at approximately 3.35 seconds, which could be considered as the boundary of Triassic shale and Ordovician fracture cavity reservoir.

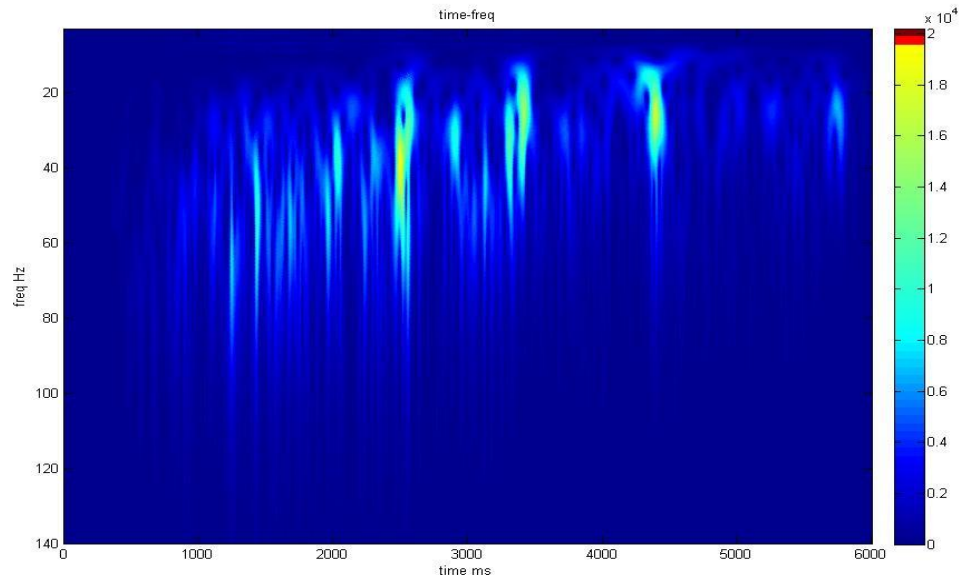


**Figure 4.4: Spectrogram for seismic trace at Well-2 location**

The spectrogram for Well-2 is shown in Figure 4.4. It is observed that the boundary information is shown at approximately 3.35 seconds, with no high energy zone at 2.4 seconds. However, one middle energy zone appears at 3.4 second in Figure 4.5 associated with water zone. Although the water zone signature is not as high as the oil zone signature at Well-1 location, it is a middle-level energy zone which appears as a bright spot in spectrogram.

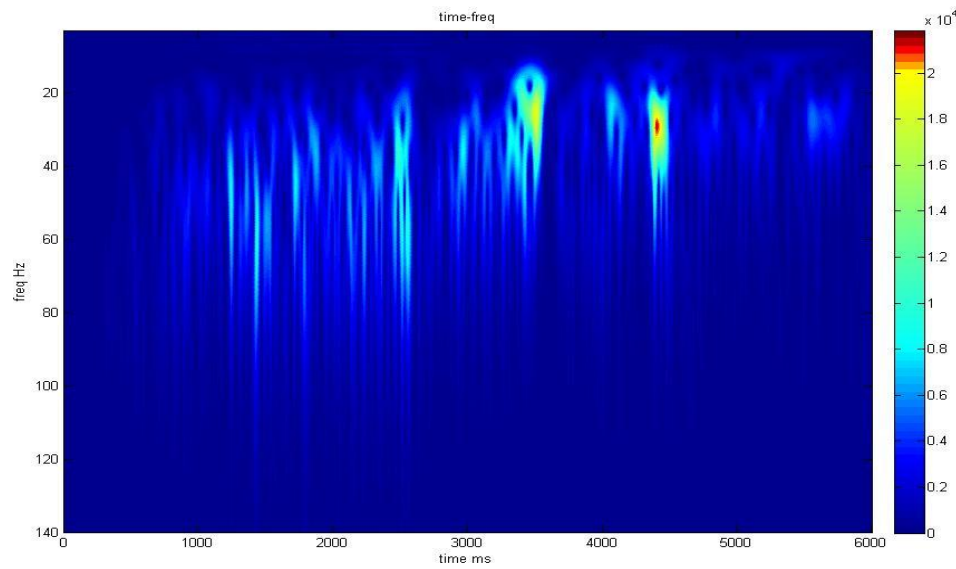


**Figure 4.5: Spectrogram for seismic trace at Well-3 location**

It is well known that it is difficult to distinguish oil from water in seismic data due to their similar physical properties. However, there is a possibility to separate the oil cave and water cave by applying wavelet analysis technique. Because this high porosity, high permeability reservoir can store large amount of fluid, the viscosity will play a significant role on oil and water separation.

#### **4.2.2 3-D seismic data analysis using wavelet transform**

Once reasonable results are obtained from single seismic trace analysis at well locations, the method can be applied to 2-D or 3-D seismic volumes. Unfortunately there is no seismic volume available for this study associated with a few seismic traces at the well locations analyzed in the previous section. Instead, I will use a second dataset that has post-stack 3-D seismic data in the same basin but different areas. The data

information is provided in Figure 4.6 and Table 4.1. By convenience, I will use 0 ms as the starting time of this data volume and 2002 ms as the ending time. The crossline number will start at 1 and end at 691. And the range for inline number will be 1 to 106.

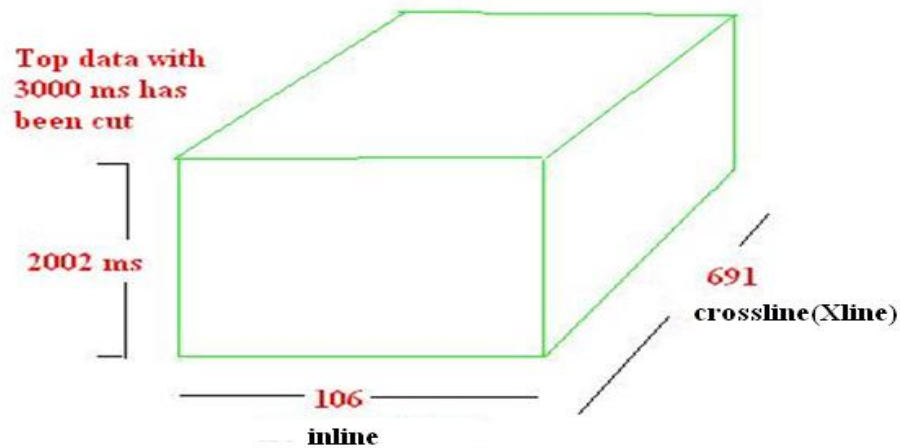


**Figure 4.6: The seismic data information**

**Table 4.1: Testing well information**

	Well -A	Well A CH	Well -B	Well B CH	Well -C	Well -D
Xline #	484	484	621	621	111	53
inline #	56	56	19	19	44	65
Bottom(ms)	840	830	770	770	890	895
Production	Water	Oil	Water	Oil	Oil	Oil

Ordovician fracture cavity reservoir is also the main target zone in the second data set. The information for four wells have been provided in this region, Well-A, Well-B, Well-C and Well-D (Table 1). Well-A and Well-B are more complex while the other



two wells have oil production at the well bottom, namely the top of Ordovician carbonate reservoir at a depth of about 6300 meters below the surface. The exploration team only found water with floating oil at Well A location when they first drilled this well. However, another team got oil production when they drilled a horizontal well several years later, which was identified as Well-A-CH. Well-B had almost the same situation as Well-A. Therefore, the complexity at the bottom of Well-A location makes this well a perfect testing well for wavelet analysis technique.

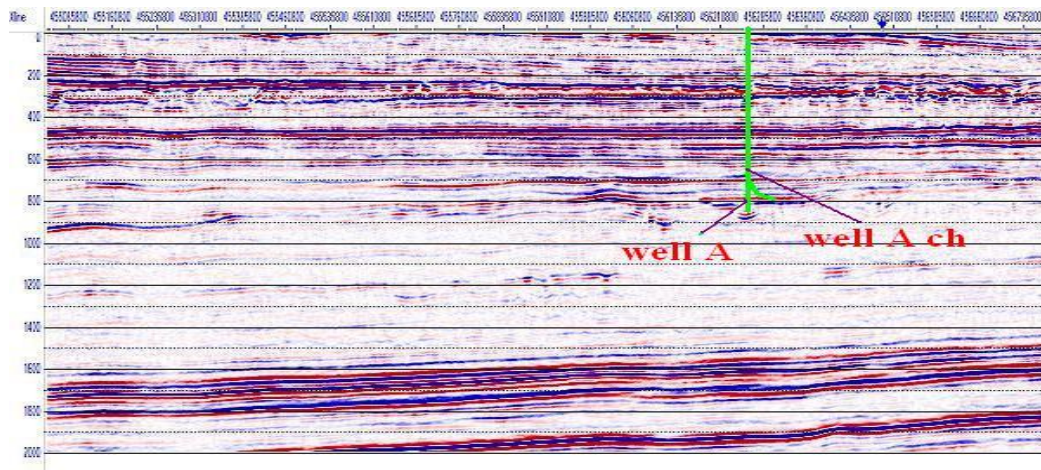


**Figure 4.7 Cross section with Well-A and Well-A-CH location information**

The Xline cross section at Well-A location is shown in Figure 4.7. This post-stack seismic data set has high S/N ratio and is considered as an amplitude-preserved seismic data set, which should provide more accurate information during wavelet decomposition process. As shown in Figure 4.8, the Ordovician fracture cavity reservoir inside the red box is the target zone for hydrocarbon exploration. Based on the seismic

amplitude cross section diagram, the green circle areas are the signature of rosary karst, which is the geological structure that potentially has hydrocarbon storage.

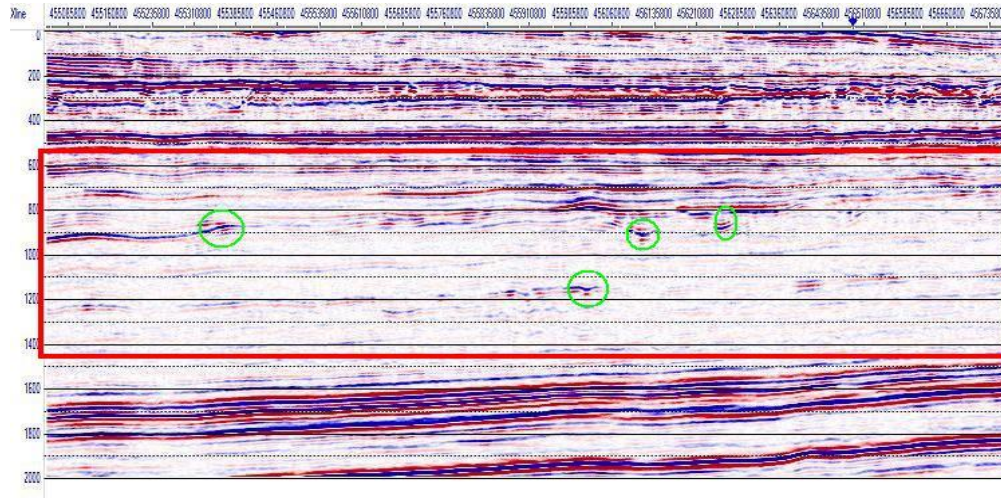


**Figure 4.8: Xline cross section with Ordovician reservoir in red box and high amplitude in green circle**

From the basic concept of the wavelet decomposition technique, it is well known that the wavelet transform has to have either high resolution in time with low resolution in frequency, or high resolution in frequency with low resolution in time at low frequency range. Therefore, the wavelet parameters should be carefully chosen so that the wavelet decomposition result could separate wave information in different frequencies while keeping a satisfied resolution in time domain at low frequency range. In order to illustrate the difference, I build a spectrogram by using  $F_c=0.2$ , and the result is shown in Figure 4.9 for selected frequency of 120 Hz. Although I got a very high resolution in time domain resulting perfect separation of the beds, the wave information

has not been decomposed at all. This spectrogram only provides the same information as the seismic data amplitude cross section diagram. Therefore, an appropriate center frequency needs to be chosen for further studies. The mother wavelet with  $F_c=1$  will be applied to this data. And the cross section and time slice spectrograms will be constructed with  $F_c=1$ .

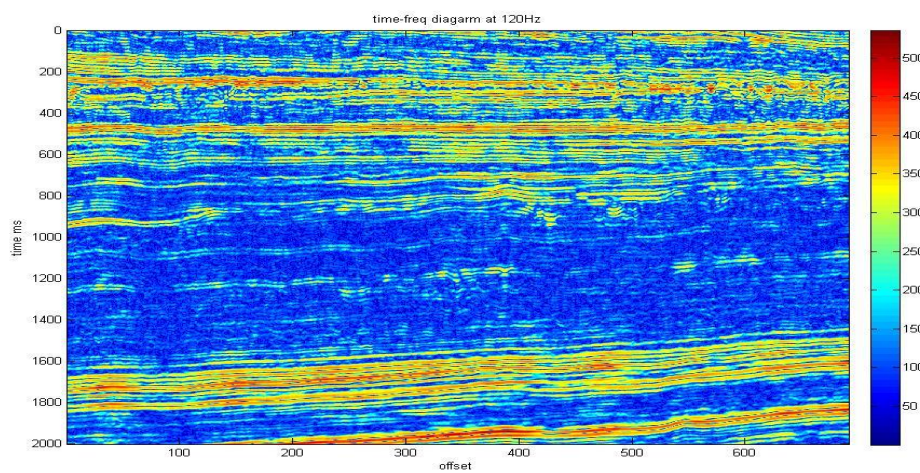


**Figure 4.9: Cross section spectrogram with using  $F_c=0.2$**

Cross section spectrograms with different frequencies can be generated by applying wavelet transform to the seismic data volume, two of which are shown in Figure 4.10 and Figure 4.11. From the cross section spectrogram at 20 Hz, it is observed that the energy at the bottom of Well-A is relatively low comparing with the top values. And the energy level at the Well-A-CH bottom is relatively high. Based on the production data, Well-A only produces water while Well-A-CH has oil production. Therefore, this indicates that wavelet transform might enable separation of oil zones



from water zones in Karst reservoirs in favorable circumstances (Vasilyev, Yuen and Podladchikov, 1997).

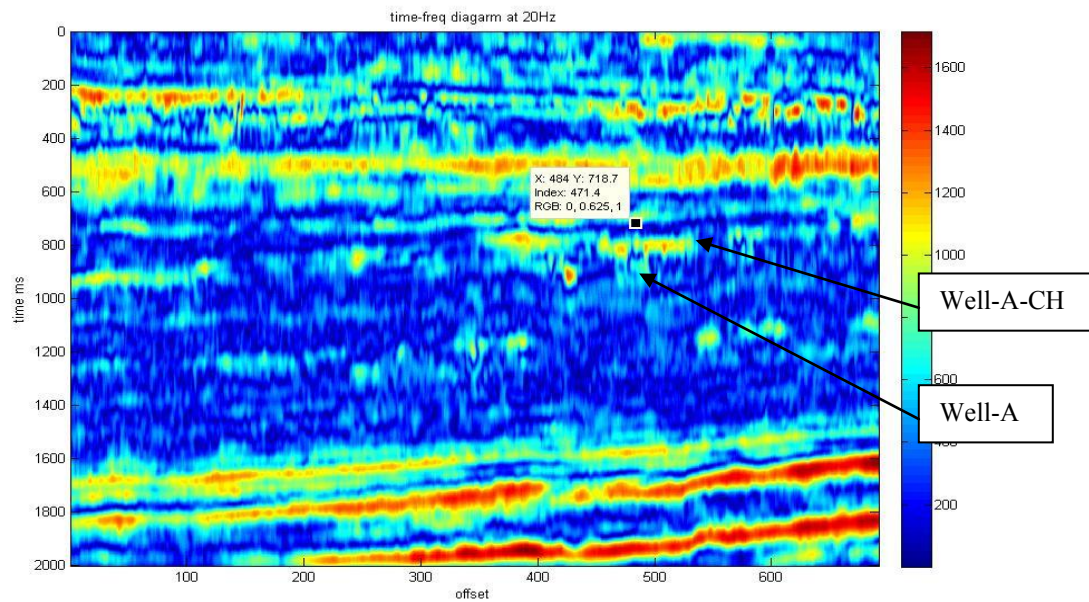


**Figure 4.10: Cross section spectrogram of 20 Hz with well information**

As selected frequency increases, the high energy information disappears. Only thin bed information is left in high frequency spectrogram due to high time resolution in high frequency area. The result is shown in Figure 4.11, which is decomposed to show stratigraphic information. Comparing the 70Hz spectrogram in Figure 4.11 with the Xline amplitude cross section in Figure 4.7, similar stratigraphic signatures can be observed from both profiles.

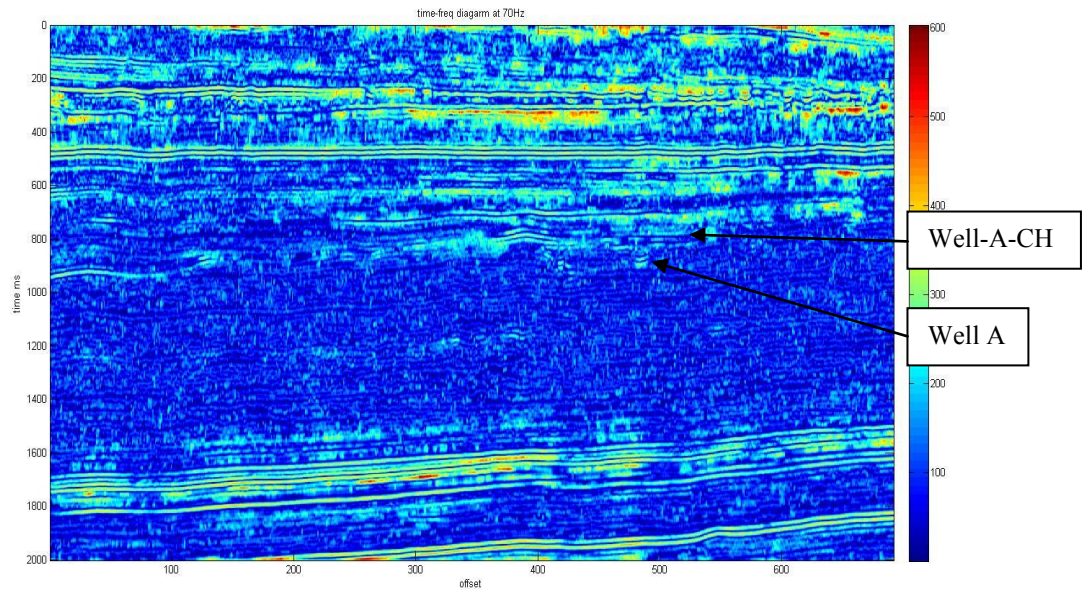


**Figure 4.11: Cross section spectrogram of 70 Hz with well information**

Although results from analysis of the crossline cross section spectrograms agree with production information, further evidence is needed both from inline cross section spectrograms and map-view spectrograms. It is expected that no high energy zones should be shown in inline cross section spectrogram at Well-A location, and high energy zones next to Well-A location in map view spectrogram.

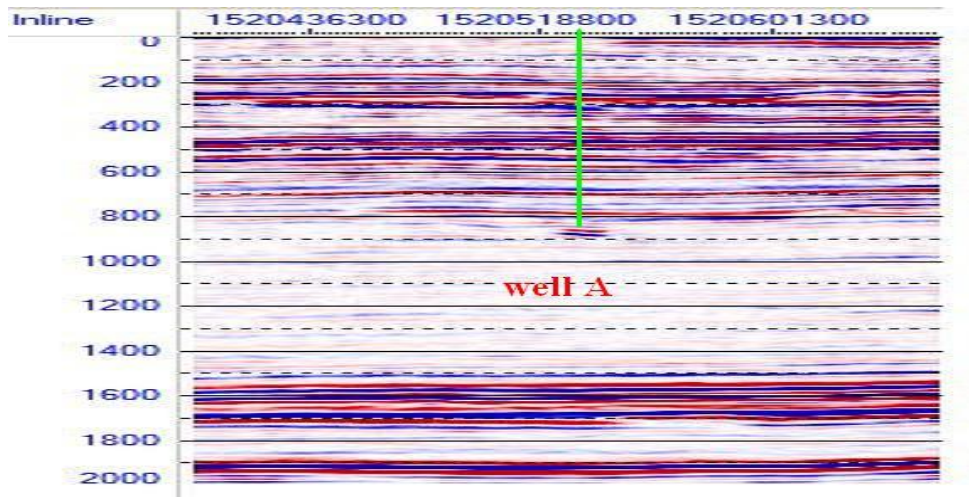


**Figure 4.12: Inline cross section with Well-A location information**

The inline seismic amplitude cross section diagram is shown in Figure 4.12. There is a signature of rosary karst at the bottom of Well-A in this amplitude cross section diagram. However, the energy of Well-A bottom is relatively low in inline cross section spectrogram at 20 Hz (Figure 4.13). As the frequency increases, the stratigraphic information becomes the major information and the signature of rosary karst appears at the high frequency end. The spectrogram with 70 Hz frequency shown in Figure 4.14 provides more stratigraphic information with less high-energy information. The difference between low frequency spectrogram and high frequency spectrogram makes the wavelet decomposition techniques a useful tool for hydrocarbon detection and stratigraphical interpretation.



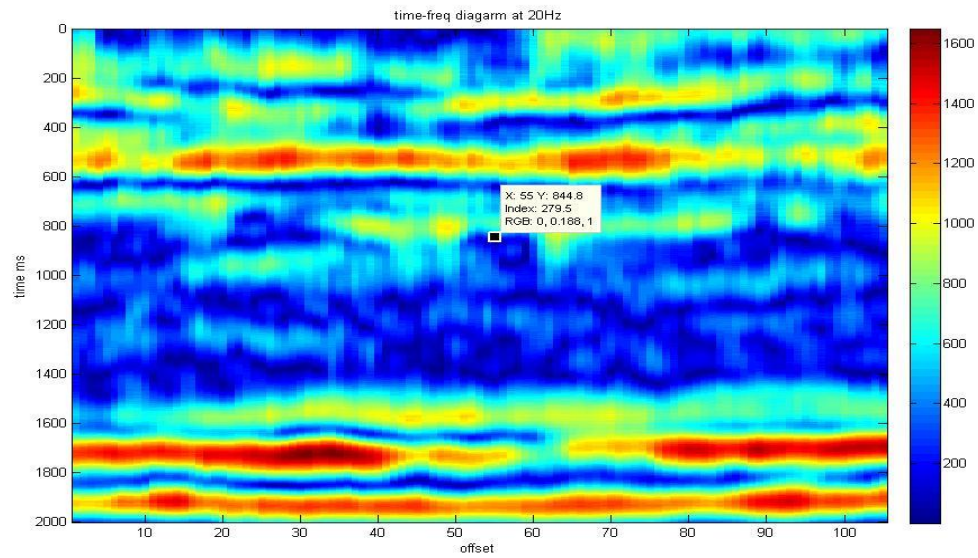


Figure 4.13: Inline cross section spectrogram of 20 Hz

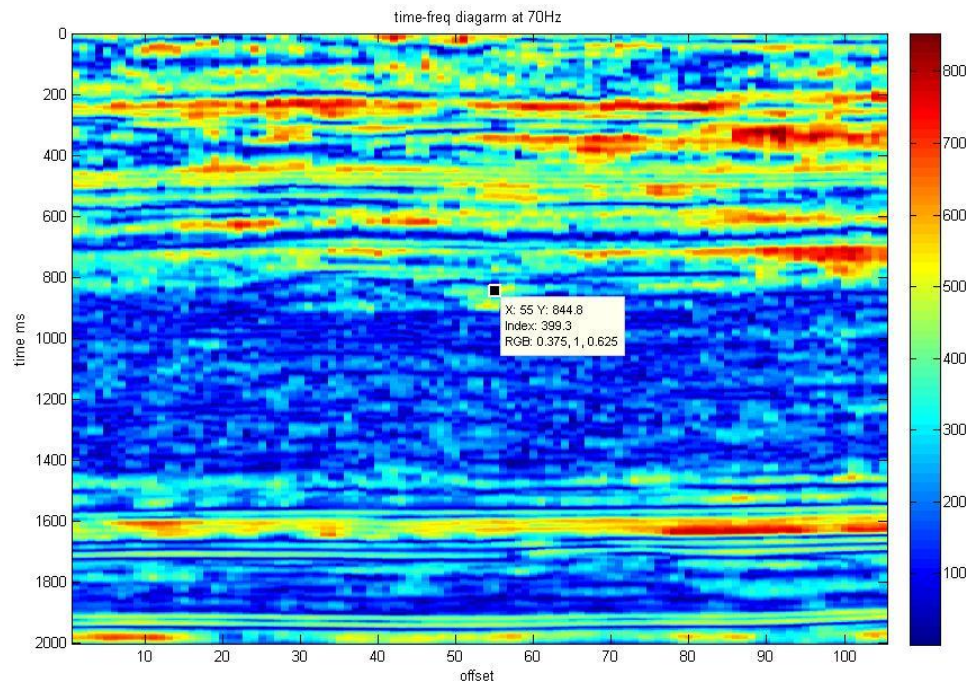
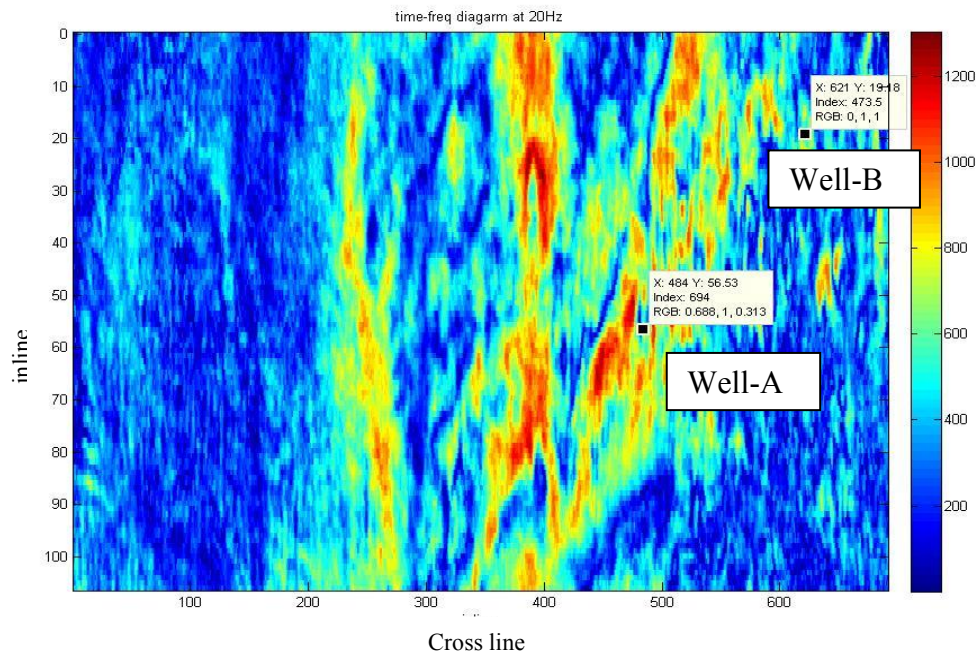


Figure 4.14: Inline cross section spectrogram of 70 Hz

Based on the well location information provided from the documents, the bottoms of Well-A and Well-B are shallower than Well-C and Well-D. The map view spectrogram slice with 20 Hz frequency at 840 ms is shown in Figure 4.15. It is obvious that the bottom of Well-A falls in to the location surrounded by high energy zones.



**Figure 4.15: Time slice spectrogram at 840 ms with 20 Hz frequency**

As depth increases, the high energy signature becomes lighter on the middle right part but a new high energy belt appears on the left side of the time slice spectrogram, where Well-C and Well-D bottoms are located, as shown in Figure 4.16. (The crossline cross section spectrograms of 20Hz, 25Hz, 30Hz, 35Hz, 40Hz, 45Hz, 50Hz, 60Hz and 70Hz are shown at the end of Chapter IV in Figures 4.17-4.25, providing the signature difference varying with frequency.)



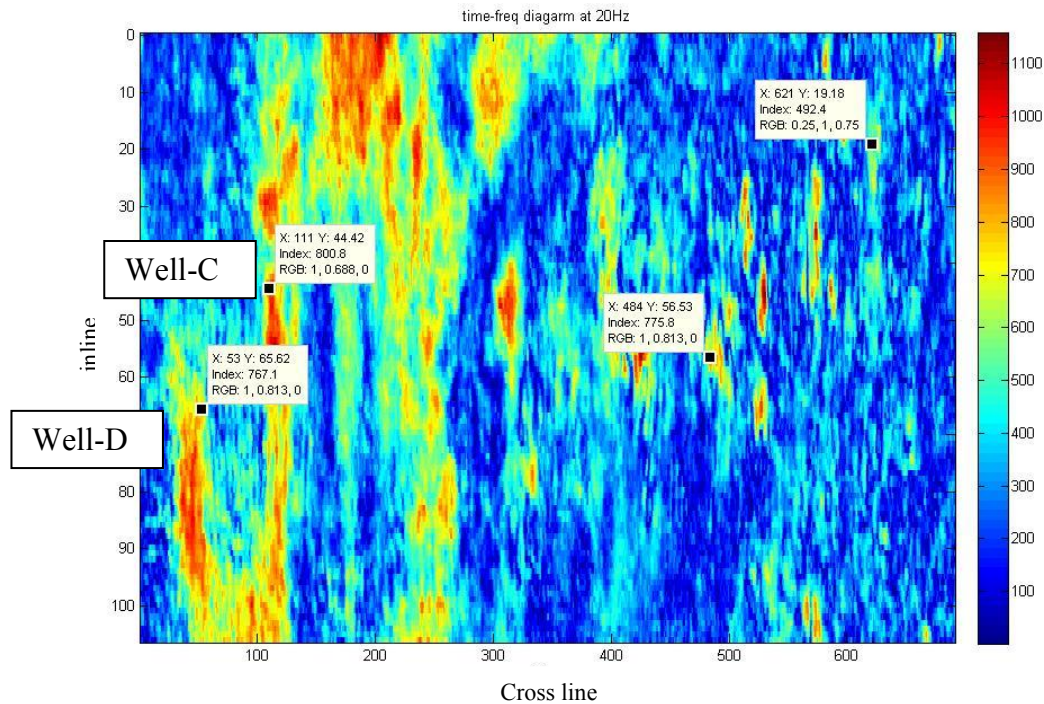


**Figure 4.16: Time slice spectrogram at 890 ms with 20 Hz frequency**

### 4.3 Conclusion

A processed 3-D post-stack seismic data set with high S/N ratio is used to test spectral decomposition using wavelet transform for an Ordovician fracture-cavity karst reservoir. This data set provides good evidence that hydrocarbon zones are detectable by using wavelet transform techniques. Results from spectrogram analysis for all of the four testing wells agree with the hydrocarbon production information provided by the drilling team. Therefore, this demonstrates that wavelet decomposition analysis technique can be used to assist geological interpretation and hydrocarbon detection, even fluid separation, in Karst reservoirs.

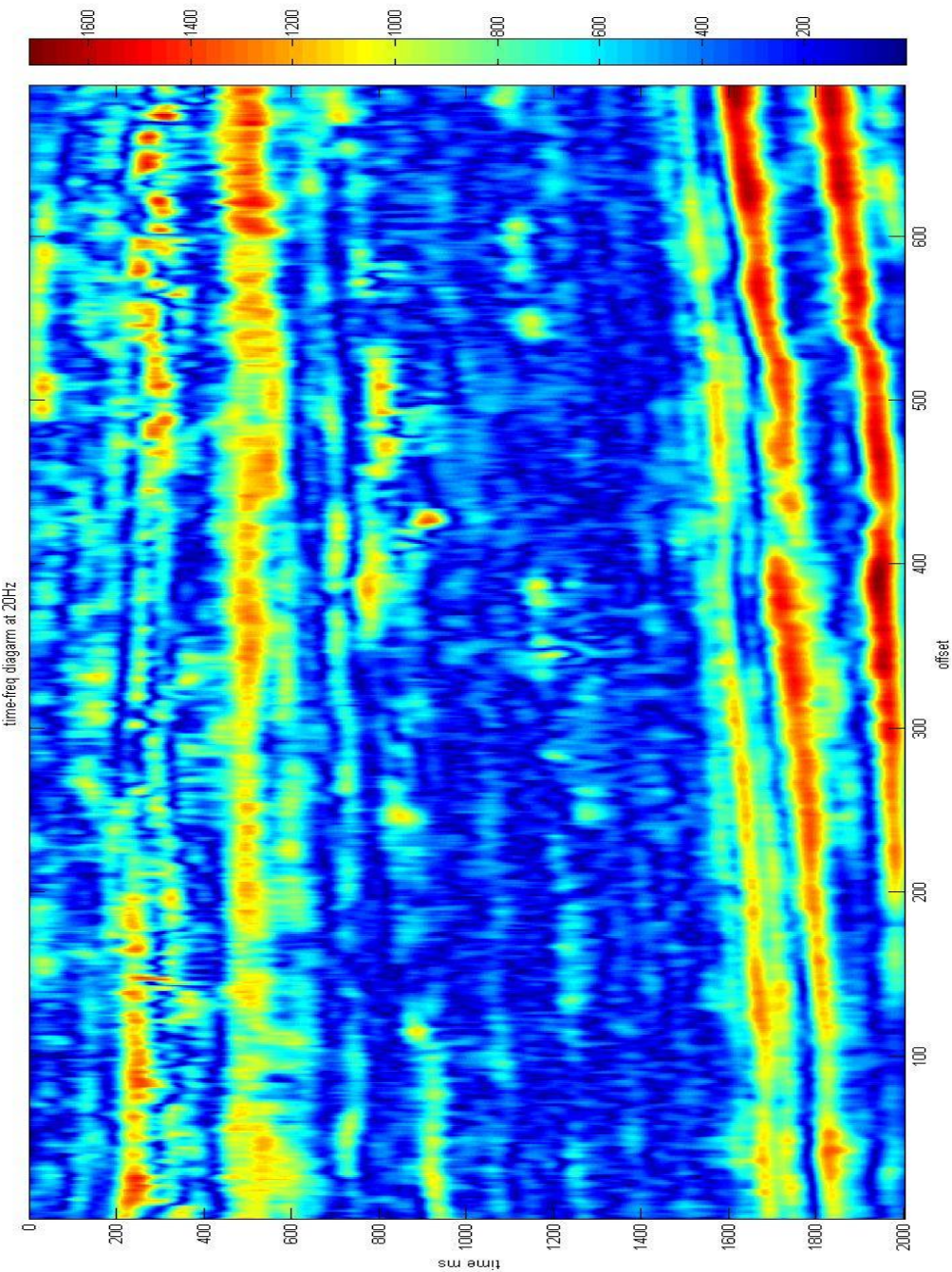
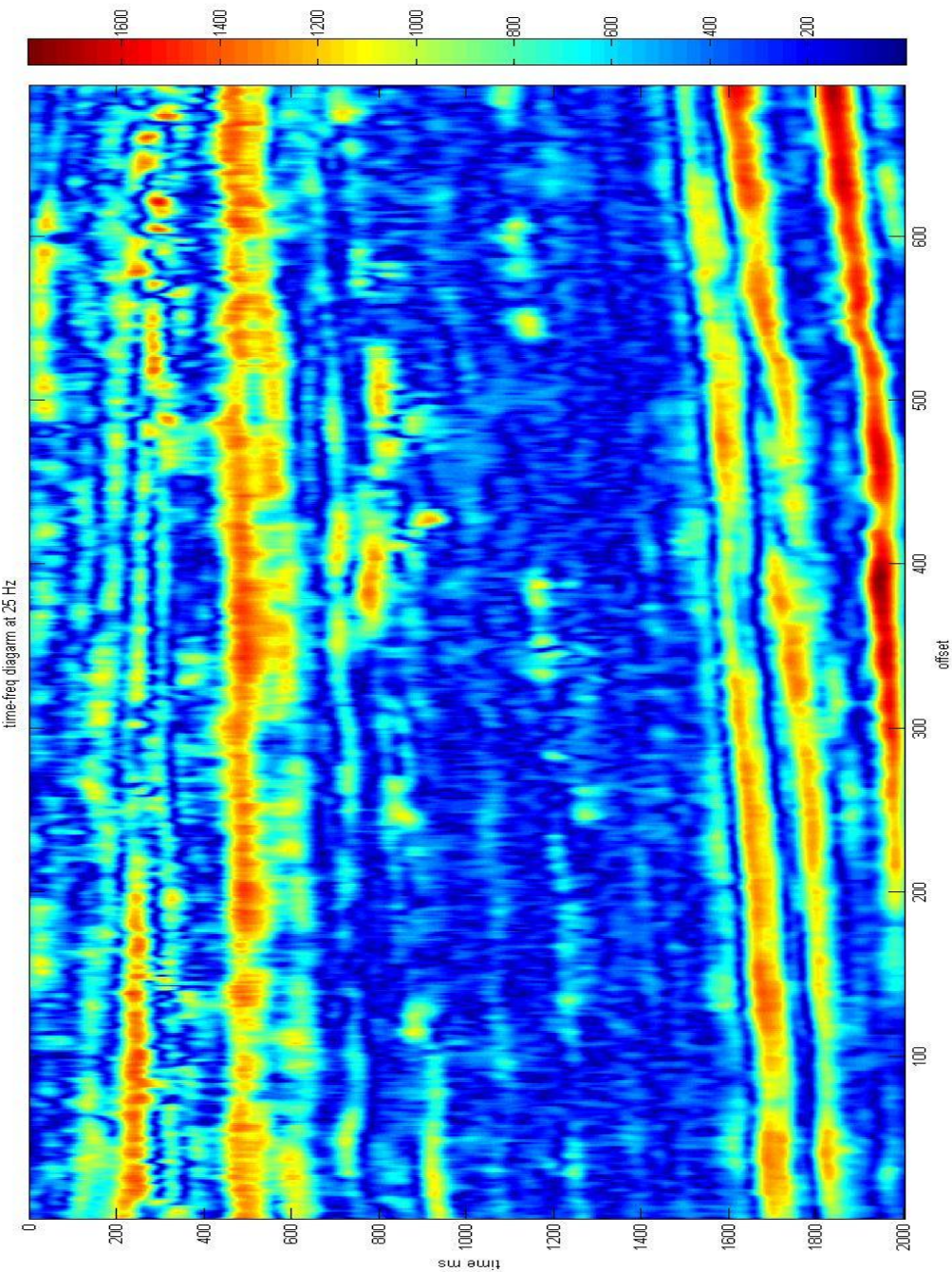
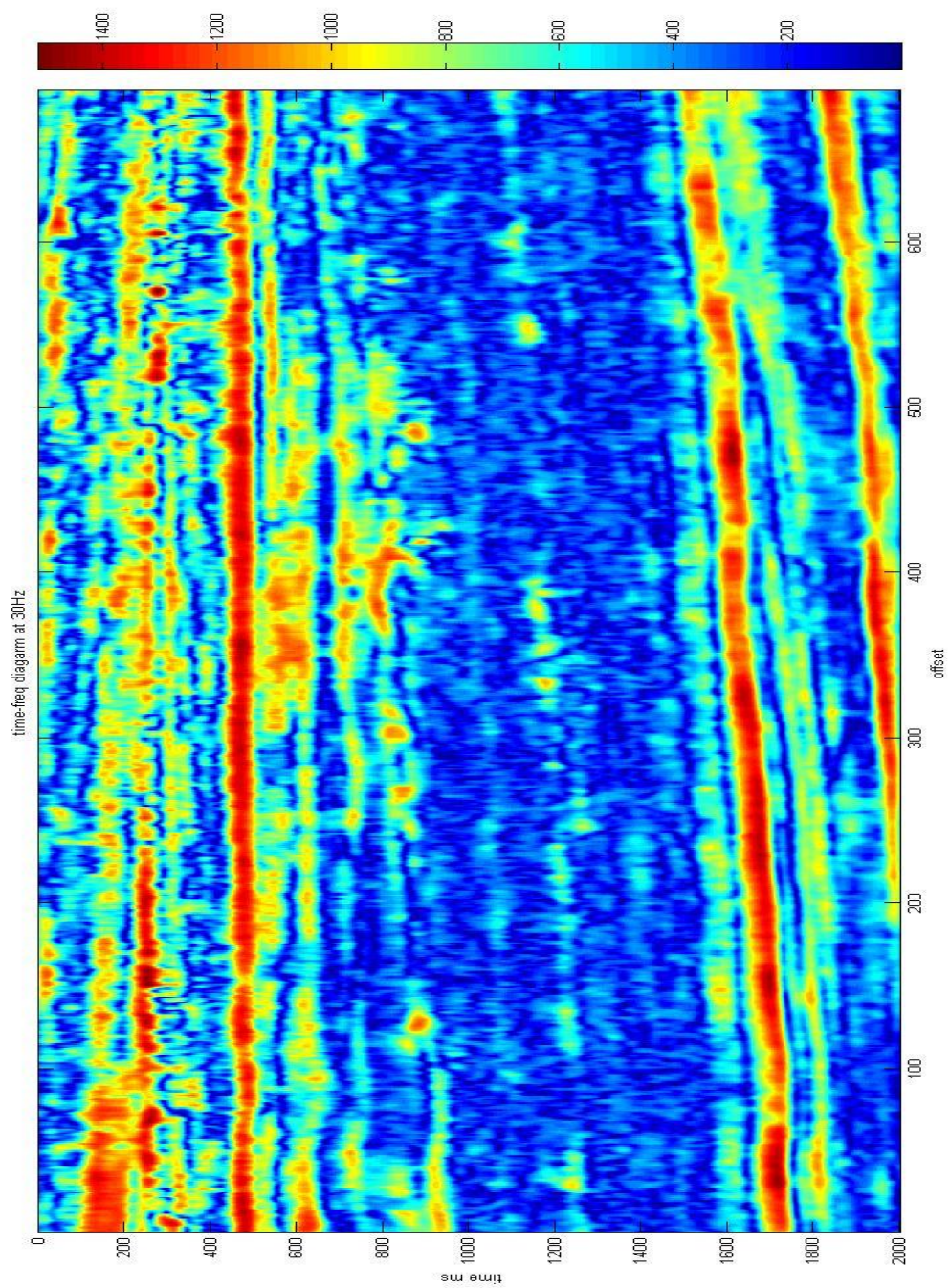


Figure 4.17: Cross section spectrogram of 20 Hz





**Figure 4.18: Cross section spectrogram of 25 Hz**



**Figure 4.19: Cross section spectrogram of 30 Hz**



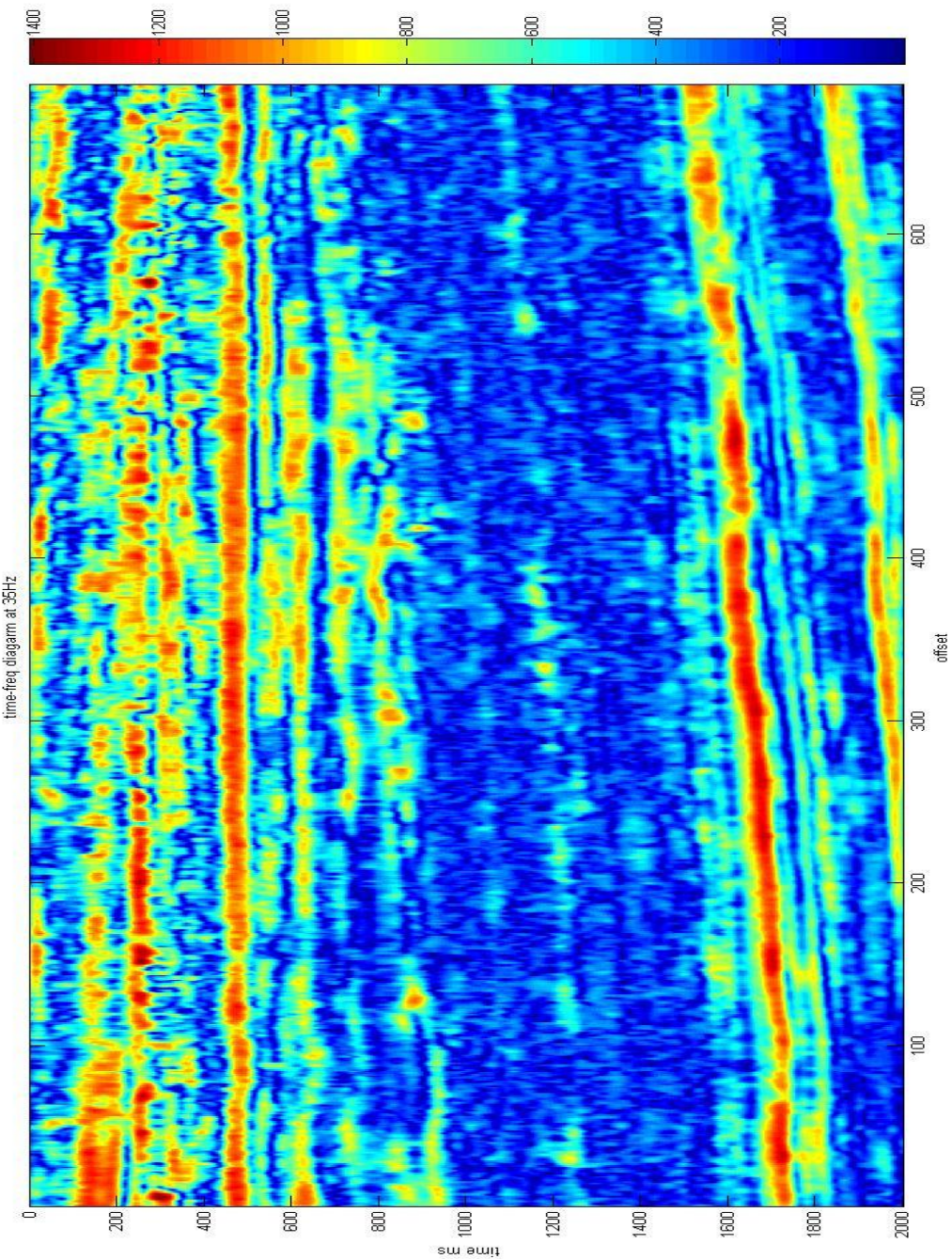


Figure 4.20: Cross section spectrogram of 35 Hz

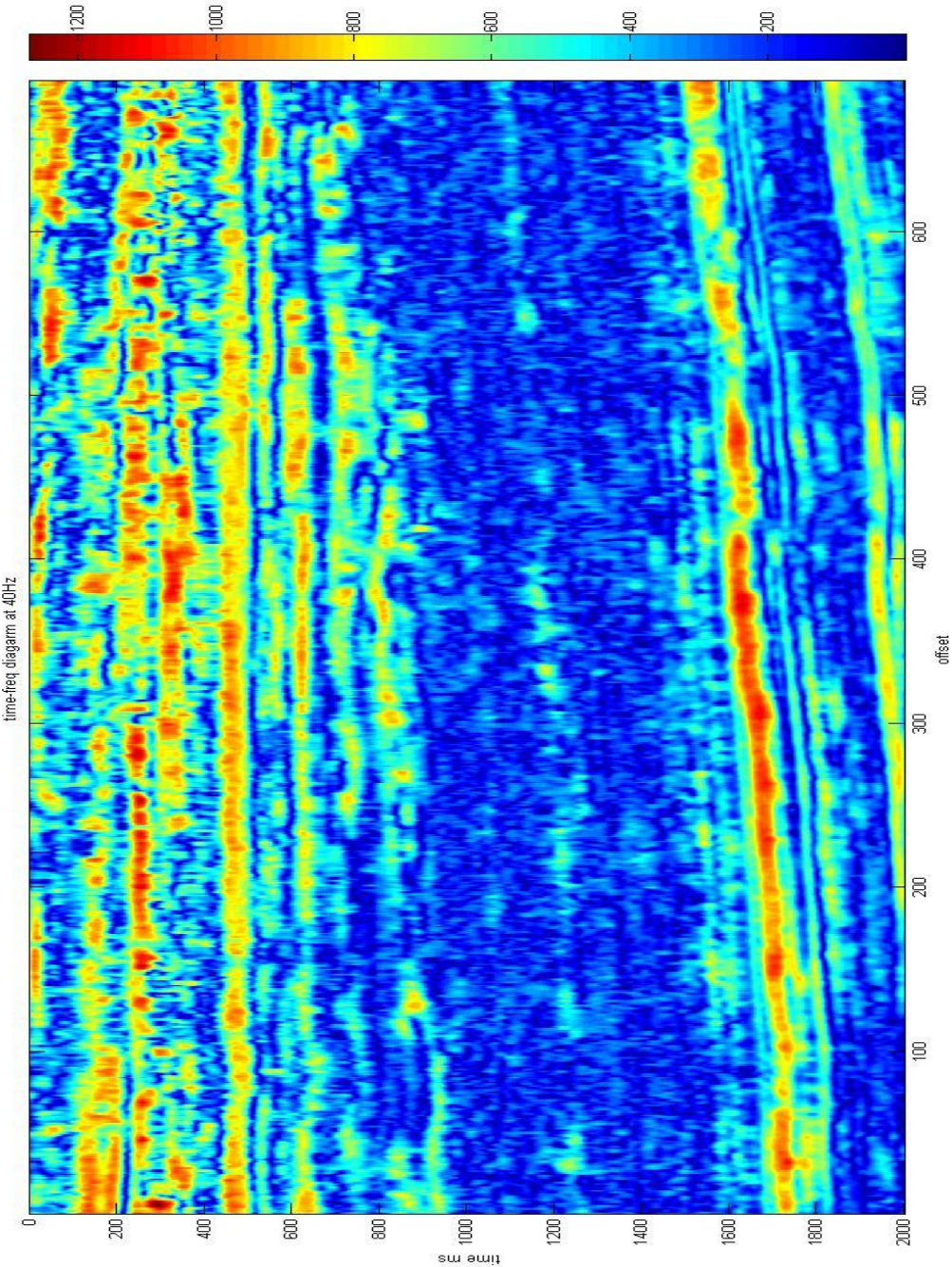


Figure 4.21: Cross section spectrogram of 40 Hz



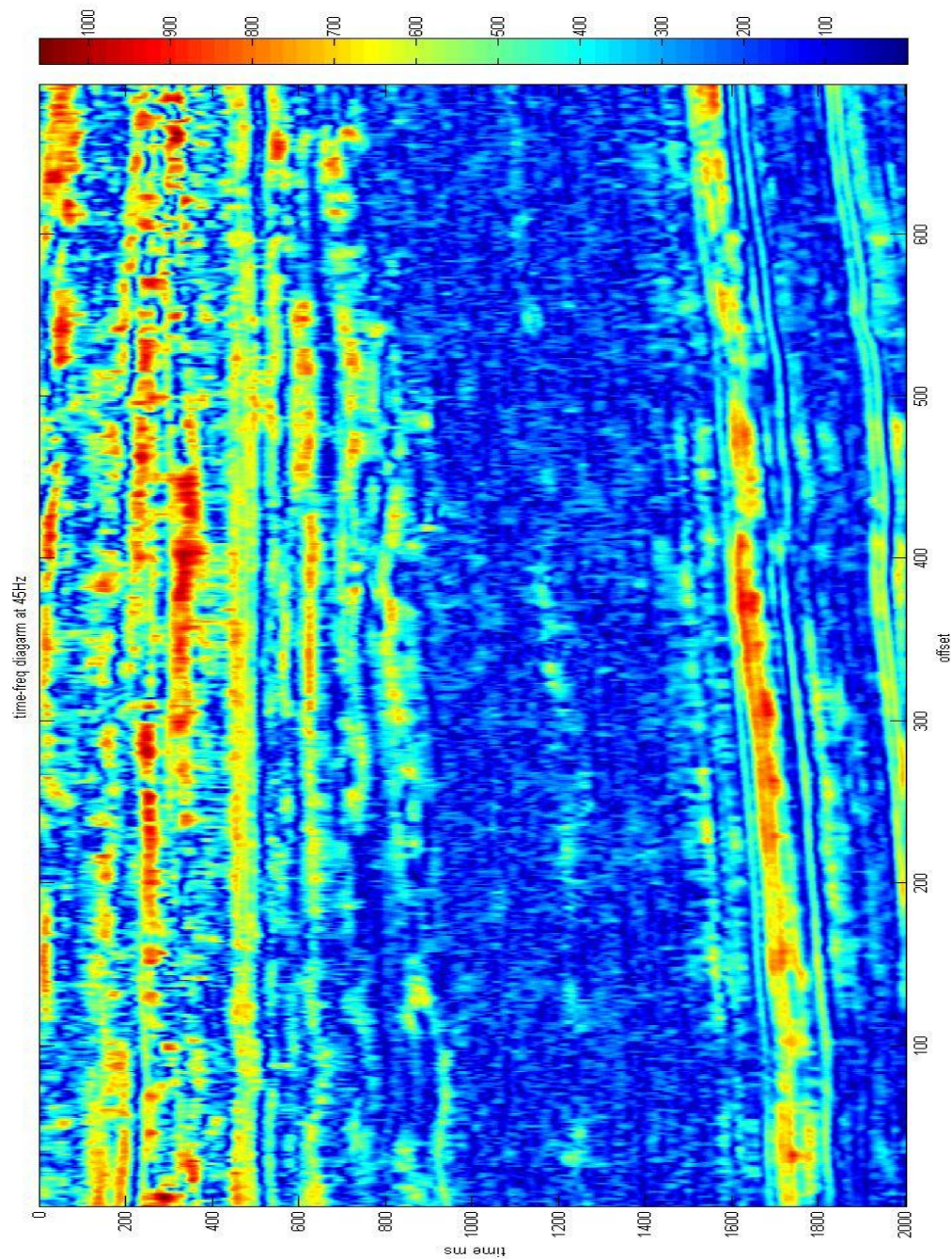


Figure 4.22 : Cross section spectrogram of 45 Hz



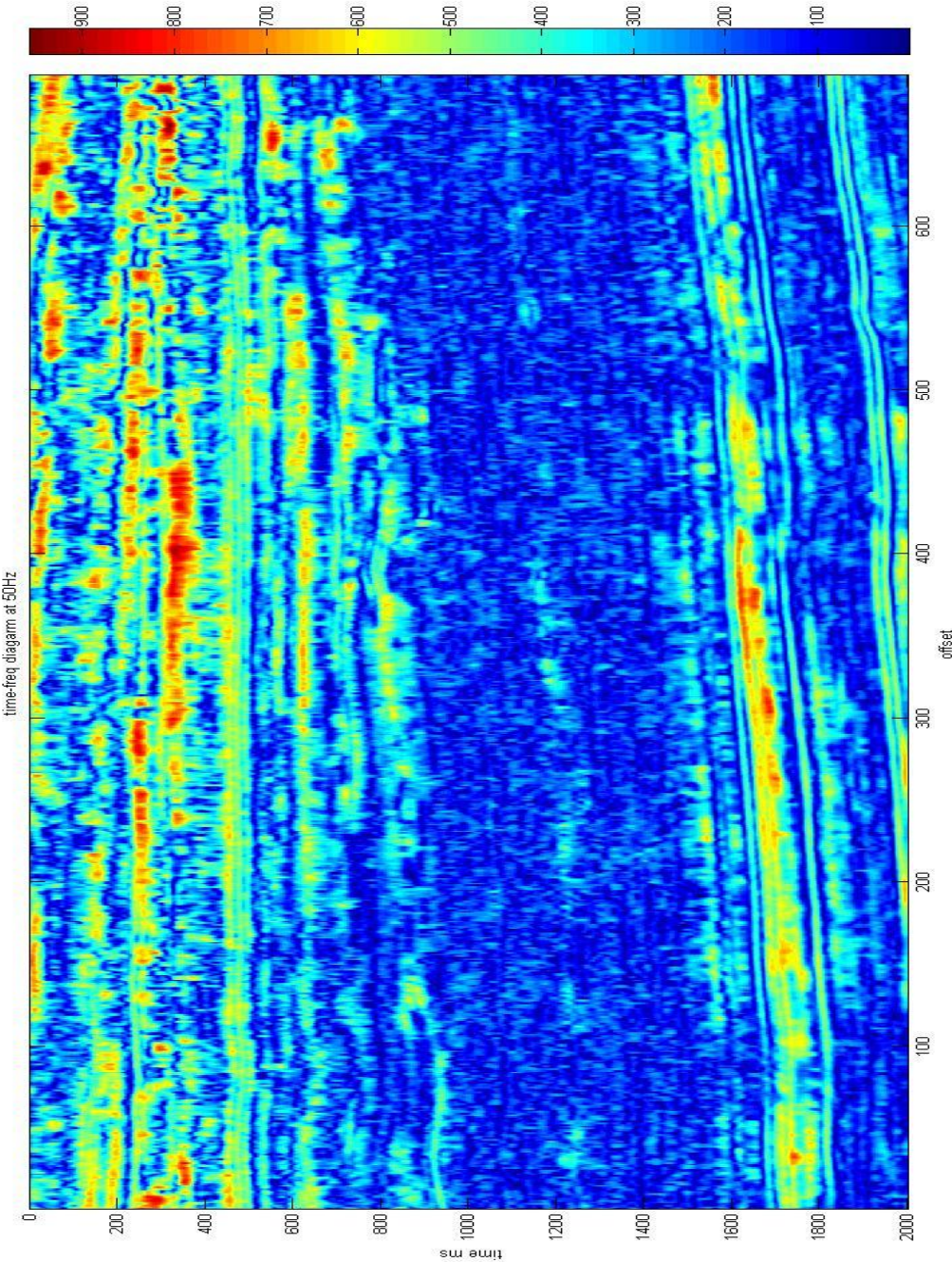
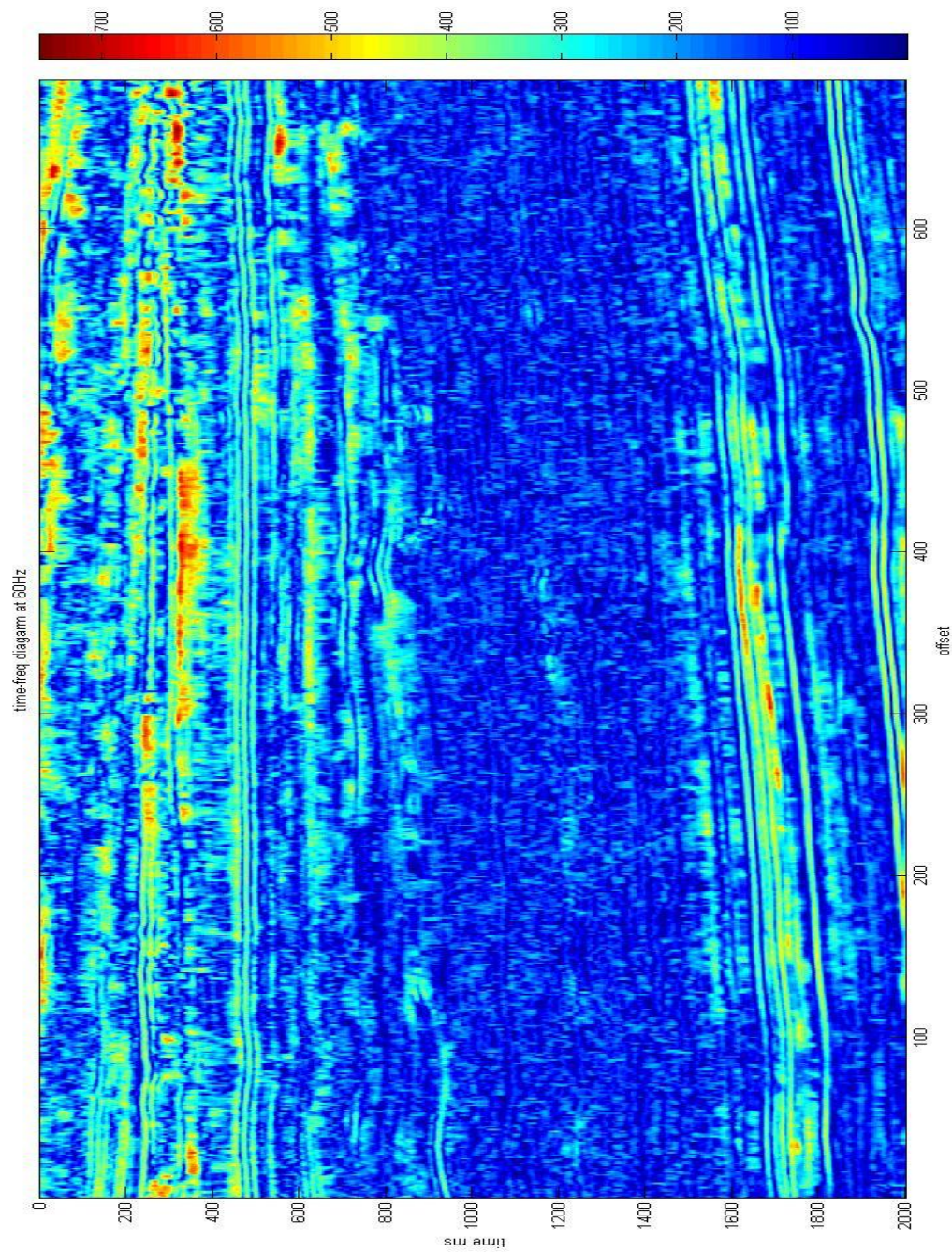


Figure 4.23: Cross section spectrogram of 50 Hz





**Figure 4.24: Cross section spectrogram of 60 Hz**



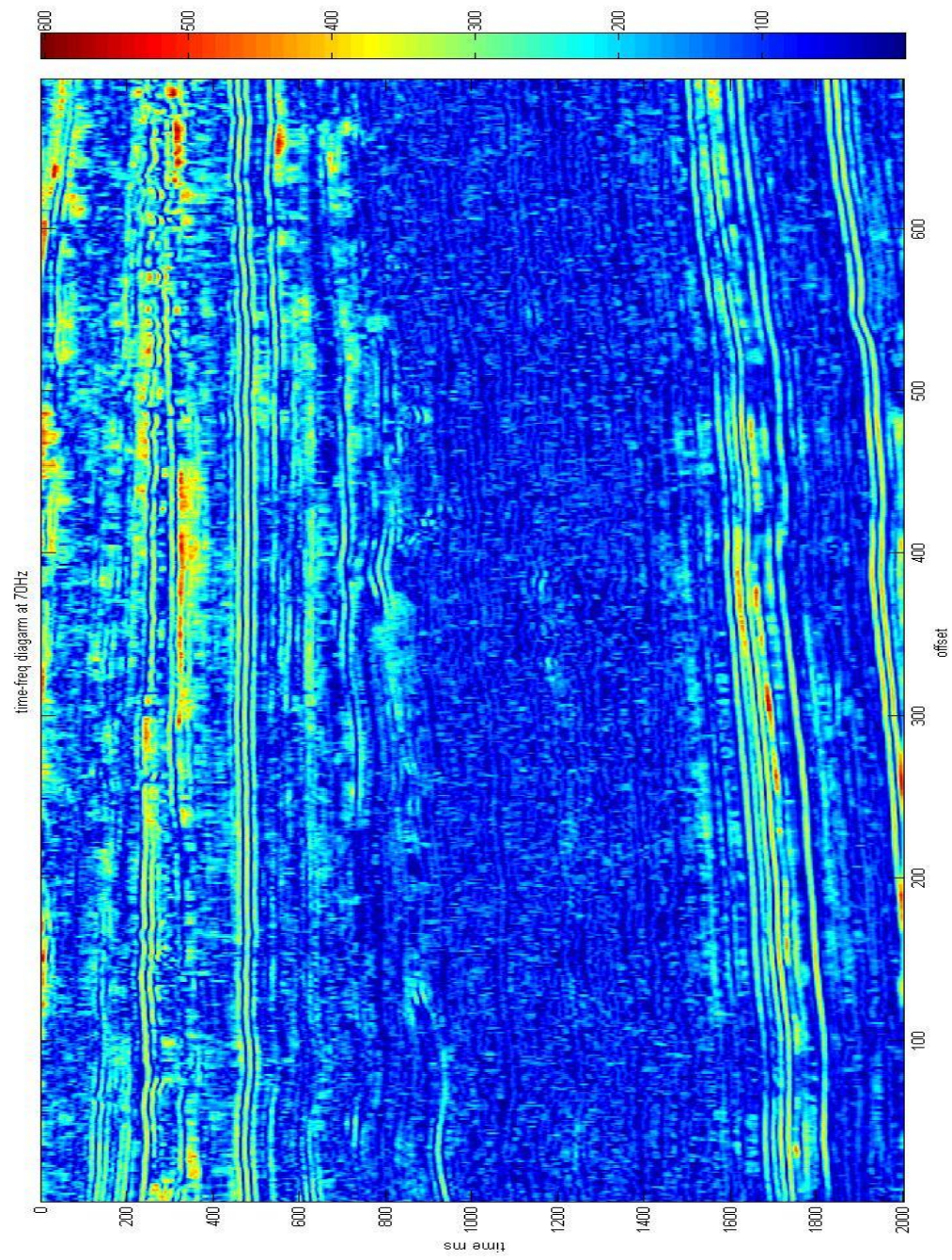


**Figure 4.25: Cross section spectrogram of 70 Hz**

## **CHAPTER V**

### **CONCLUSIONS**

It is often observed in the field that seismic wave undergoes significant changes when it propagates through a hydrocarbon reservoir. One of the new techniques to detect such changes is wavelet decomposition which enables analysis of wave information in different frequencies. My research in this study is to investigate the validity of wavelet decomposition analysis for hydrocarbon detection in both clastic and carbonate environments.

Although Fourier transform, short-time Fourier transform and wavelet transform all can be used for wave decomposition analysis, the wavelet transform could be a better method due to its ability of handling the non-stationary seismic waves. The selection of the mother wavelet is significant for wavelet decomposition process. Furthermore, the parameter for mother wavelet should be chosen appropriately so that the resolution in both frequency and time could be optimized simultaneously.

For the studied clastic reservoirs from the North Sea, results of wavelet decomposition analysis agree with the known information at well locations for both synthetic seismic traces and real seismic traces. Because this seismic data set is from unprocessed shot gathers, results have been compromised by multiples and noise. However, high energy zones associated with known hydrocarbon occurrences can still be observed at low frequency from the cross section spectrogram, and shallow beds can be identified at high frequency range. Therefore, wavelet analysis proves to be a useful

tool to assist geological interpretation and hydrocarbon detection for the clastic reservoirs. However, further study with high-quality 3-D seismic data is recommended to provide more evidence for application of wavelet decomposition analysis technique to clastic environments.

Wavelet decomposition analysis has also been successfully applied to study karst fracture-cavity reservoirs, with high-quality seismic data sets available for this study. Results from analysis of the spectrograms obtained from Xline cross section, inline cross section and time slice agree with production information at well locations. It seems that the oil and water separation can also be achieved in the studied Karst reservoir.

There are, however, still some limitations in wavelet decomposition analysis techniques. First of all, the parameters for mother wavelet should be carefully chosen to obtain satisfactory resolution in both frequency and time. Secondly, the signal-to-noise ratio of the seismic data used for wavelet decomposition should be reasonably high and the data should have multiples be removed. Thirdly, although this technique could separate oil from water in karst reservoirs as in this study, there may not be sufficient differences to separate oil from water for thin-bedded reservoirs due to the density similarity of oil and water.

Despite of its limitations, wavelet decomposition analysis technique as proposed and studied in this research shows a great potential to lower the risk in hydrocarbon exploration. It can be directly applied to processed 2-D and 3-D pre-stack/post-stack data to detect hydrocarbon zones in low frequency range and identify shallow thin beds in high frequency range for both clastic and carbonate reservoirs. Therefore, Use of

wavelet decomposition analysis combined with AVO analysis could provide better and more accurate means for seismic interpretation and hydrocarbon detection.

## REFERENCES

- Goff, J. C., 1983, Hydrocarbon generation and migration from Jurassic source rocks in the E Shetland Basin and Viking Graben of the North Sea, J. Geol. Soc. London, Vol. 140, p.445-474.
- Goswami, J. C., and A. K. Chang, 1999, Fundamental of wavelets – theory, algorithms, and applications: John Wiley & Sons Inc.
- Goupillaud, P., Grossman, A., and J. Morlet, 1984, Cycle-octave and related transforms in seismic signal analysis. *Geoexploration*, 23:85-102.
- Keys, R. G., and D. J. Foster, Single, 1998, Comparison of seismic inversion methods on a single real data set, Mobil Exploration & Production technical center.
- Lang, C. W., and K. Forinash, 1998, Time-frequency analysis with the continuous wavelet transform, Indiana University Southeast.
- Liu, P. C., and G. S. Miller, 1996, Wavelet transform and ocean current data analysis, *Journal of atmospheric and oceanic technology*, Vol. 13, abstract.
- Loucks, R. G., and C. R. Handford, 1992, Origin and recognition of fractures, breccias, and sediment fills in paleocave-reservoir networks, *Society of Economic Paleontologists and Mineralogists Publication* 92-33, p. 31-44.
- Pegrum, R. M., and A. M. Spencer, 1991, Hydrocarbon plays in the northern North Sea: London, Geological Society, Special Publication 50, p.441-470.
- Ren, C., Weiland, P., and X. Xiao, 2003, Application of a modified morlet wavelet in feature extraction, Vol 18, No. 6.

- Sato, H., 1997, Energy propagation including scattering effects single isotropic scattering approximation, National Research Center for Disaster Prevention, J. Phys. Earth, 27-41.
- Singleton, S., Taner, M. T., and S. Treitel, 2006, Q estimation using gabor-morlet Joint time-frequency analysis techniques, TriDekon Inc, SEG abstract.
- Sinha, S., 2002, Time-frequency localization with wavelet transform and its application in seismic data analysis: Master's thesis, University of Oklahoma.
- Sinha, S. K., Routh, P. S., Anno, P. D., and J. P. Castagna, 2003, Time-frequency attribute of seismic data using continuous wavelet transform, SEG Abstract, 2003.
- Sun, S., and J. P. Castagna, 2006, Comparison of spectral decomposition methods, first break volume 24.
- Vasilyev, O. V., Yuen, D. A., and Y.Y. Podladchikov, 1997, Applicability of wavelet algorithm for geophysical viscoelastic flow, Geophysical research letters, Vol. 24, No. 23, p. 3097-3100.
- Yang, J., Xiao, Y., and G. Peng, 2009, Application of well-driven seismic in tazhong area, Tarim Oilfield Company PetroChina, SEG abstract, Beijing.
- Zabihian, N. E., and H. R. Siahkookhi, 2006, Single frequency seismic attribute based on short time fourier transform, continuous wavelet transform and s transform, University of Tehran, International conference of geophysics abstract.

## VITA

Rui Cai received his Bachelor of Science degree in electrical engineering from Texas A&M in 2004. He entered the geophysics program at Texas A&M University in September 2008 and will receive his Master of Science degree in December 2010. His research interests focus on seismic analysis using wavelet transform decomposition for hydrocarbon detection.

Name: Rui Cai

Address: Department of Geology and Geophysics

MS 3115, c/o Dr. Yuefeng Sun

Texas A&M University, College station, TX 77843-3115

Email Address: no8cai@tamu.edu

Education: B.S., Electrical Engineering, Texas A&M University, 2004

M.S., Geophysics, Texas A&M University, 2010